NATIONAL AERONAUTICS
AND SPACE ADMINISTRATION

NASA Contract NASr-36

TRANSIENT PRESSURE MEASURING METHODS RESEARCH

AN ANALYTICAL AND EXPERIMENTAL STUDY OF THE RESPONSE OF A SMALL CHAMBER TO FORCED PRESSURE OSCILLATIONS

Aeronautical Engineering Report No. 595d

Prepared by: Clifton L. Carwile
Clifton L. Carwile
Assistant in Research

Approved by: J. P. Layton
J. P. Layton
Research Leader

15 October 1962

Guggenheim Laboratories for the Aerospace Propulsion Sciences
Department of Aeronautical Engineering
PRINCETON UNIVERSITY

ACKNOWLEDGMENTS

The work described herein was carried out as an MSE thesis by the author as a part of a broad research (JP-24) on transient pressure measuring methods in the Research Program of The Guggenheim Laboratories for the Aerospace Propulsion Sciences, Department of Aeronautical Engineering, Princeton University. Support of this thesis under a contract (NASr-36) from the National Aeronautics and Space Administration is gratefully acknowledged. Some additions have been made in publishing this work as a technical report.

The author wishes to acknowledge his special indebtedness to Mr. Howland B. Jones, Jr. without whose guidance and assistance this work could not have been accomplished.

He also wishes to express his gratitude to Professor Jerry Grey who directed the course of the analytical and experimental work.

Additional thanks are due the staff of the Guggenheim Laboratories Research Program, especially Mr. Tony Poli of the Design Group, Miss Frances Allison, and the secretarial staff.

ABSTRACT

The various resonant modes of gas pressure oscillations in a Sinusoidal Pressure Generator, featuring a closed, flat cylindrical chamber, were theoretically determined and verified experimentally, using Freon-12 and nitrogen as test media.

For chamber length-to-diameter ratios less than 1.71 the transverse modes were shown to be dominant. Since the test chamber of the Sinusoidal Pressure Generator had a length-to-diameter ratio of only 0.38, it was predicted analytically that the lowest obtainable resonant frequencies would be the first and second tangential modes. Strong transverse nearly-sinusoidal waves corresponding to these two modes were obtained in the tests, but with frequencies somewhat less than those predicted by acoustic theory.

In theory, a pressure transducer which has a circular diaphragm concentric with a cylindrical chamber for its sensing element will exhibit no net response to the tangential ("sloshing") modes. Such a transducer mounted in the end wall of the chamber did, indeed, not respond to these modes. The theory was then extended to cover plane waves moving parallel to the diaphragm face, and predicted an amplitude decrement and increased phase shift as the frequency increased.

The Sinusoidal Pressure Generator was evaluated for its designed function of determining pressure transducer frequency response. With helium as the test gas the character of the pressure waves were shown to be essentially sinusoidal and the amplitudes of the oscillations were adequate for transducer testing throughout a test range from 1,800 to 21,600 cps. However, a departure from uniform sinusoidal response was apparent as the frequency was increased, limiting the applicable range of the Sinusoidal Pressure Generator as currently designed to about 10,000 cps for pressure transducer evaluation.

TABLE OF CONTENTS

NOMENCLATURE

A = area

A = scale factor for amplitude of sinusoid

a = chamber radius

c = velocity of wave propagation

d = chamber diameter

e = constant having the value 2.7128 ...

f = frequency

g = conversion factor, 32.17 ft/sec/sec

i = complex quantity, $\sqrt{-1}$

J = Bessel function

K = a constant

L = chamber length

M = subscript indicating a mean value

M_o = molecular weight

m_h = unit of inductance

m = running index equal to 0, 1, 2, 3, ...

n = running index equal to 0, 1, 2, 3, ...

n_z = running index equal to 0, 1, 2, 3, ...

p = pressure

Q = sharpness of resonance

R = radius of a transducer diaphragm

R = gas constant

R_o = universal gas constant

r = radial space coordinate in cylindrical coordinates

T = absolute temperature

t = time variable

NOMENCLATURE (Continued)

w = variable equal to x/R, where R = diaphragm radius

X = intercept of Lissajous pattern on oscilloscope

x = Cartesian coordinate

Y = maximum height of Lissajous pattern on oscilloscope

y = Castesian coordinate

z = coordinate in cylindrical coordinates

α_{mn} = solution of $dJm\,(\pi\alpha_{mn})/d\alpha = 0$

γ = ratio of the specific heats

μf = unit of capacitance

φ = angular coordinate in cylindrical coordinates

ϕ = phase angle

ω = angular velocity

Ω = unit of resistance

ν = resonant frequency

LIST OF FIGURES

I. INTRODUCTION

One commonly-used method of determining transducer performance has been to analyze the response to a step pressure input generated by a shock tube. It is relatively simple to determine the natural frequency (assuming low damping) by counting the number of cycles of oscillation during a known time period. The damping ratio can be determined from the number of oscillations occurring prior to decay to 50% amplitude. See (1)*, Figure 3.

Tallman (2) also developed a method for obtaining the complete frequency response from shock tube data by using Guilleman's impulse technique. The method is difficult to apply and the resultant frequency response has a jagged, irregular appearance.

In addition to the difficulty of data analysis, there are some problems peculiar to shock tube testing. The transducer is subject to "ground shock" through the transducer mount and the transducers may be affected nonlinearly by the acceleration of the diaphragm due to the impinging shock front. These factors will tend to obscure the response to a pure step pressure input and to complicate the analysis.

Flow throttling devices with sinusoidal pressure oscillations permit direct determination of the frequency response without involved data analysis and sophisticated instrumentation. Although attractive in theory, flow throttling devices in the past have demonstrated either inadequate amplitude in the desired frequency range or nonsinusoidal wave shapes. The generator described in this report, although falling into this general category, was successful in eliminating these

---

*Numbers in parentheses indicate references at end of report.

difficulties, as will be described later.

In short closed cylinders such as the test chamber in the present generator, the transverse modes are dominant at resonance. Although discussed quite thoroughly theoretically, little has been done experimentally to produce these modes. Morse (3) discusses the standing waves in a cylindrical room, and much of the analytical work in this report is an extension of his work. This is an acoustic resonance in which the frequency is independent of the pressure amplitude.

Maslen and Moore (4) developed a theory for strong transverse waves in a circular cylinder and showed that the frequencies at resonance were influenced by the strength of the wave, but that for waves of moderate strength the frequencies were close to those of the acoustic modes. They also concluded that the frequency of a strong transverse wave is less than that of the associated acoustic mode, and that strong transverse waves do not steepen into shocks.

II. PURPOSE AND METHOD OF APPROACH

The purposes of the tests were twofold:

1. To investigate the transverse modes of chamber resonance.

2. To evaluate the usefulness of the pressure generator as a transducer testing device.

The resonant modes of the chamber were investigated first theoretically and then experimentally. The test gases for this phase were Freon-12 and nitrogen, which were used in order to bring some of the theoretical resonance frequencies within the operating range of the generator. The response to transverse resonant modes of a test transducer having a large diaphragm as a sensing element was investigated analytically and experimentally.

The chamber response was then determined at discrete frequencies throughout the operating range of the generator, using three small quartz transducers placed at various locations on one end wall of the cylindrical test chamber. For transducer testing it is desirable that the response be uniform and sinusoidal throughout the chamber. Helium was the test gas used for this phase.

III. ANALYTICAL STUDY

The following section considers theoretically the various modes of standing waves in a cylindrical chamber. In addition to describing the resulting pressure patterns, application is made to predict the integrated response of a transducer to the various modes.

A. Theoretical Chamber Resonance

The wave equation for the pressure at any point can be written in cylindrical coordinates:

$$\frac{1}{c^2}\frac{\partial^2 p}{\partial t^2} = \frac{1}{r}\frac{\partial}{\partial r}\left(r\frac{\partial p}{\partial r}\right) + \frac{1}{r^2}\frac{\partial^2 p}{\partial \varphi^2} + \frac{\partial^2 p}{\partial z^2} \qquad (1)$$

The solution to this equation is, after Morse (3), p. 398

$$p = \cos(m\varphi)\cos\left(\frac{\omega_z z}{c}\right) J_m\left(\frac{\omega_r r}{c}\right) e^{-2\pi i \nu t}, \quad \nu = \frac{1}{2\pi}\sqrt{\omega_z^2 + \omega_r^2} \qquad (2)$$

where* m = 0, 1, 2, 3, ...

c = velocity of wave propagation

ω_z, ω_r = angular velocities in z and r directions respectively

J_m = Bessel functions

ν = frequency of the pressure fluctuations

The three space coordinates z, r, and φ are defined by the following diagram.

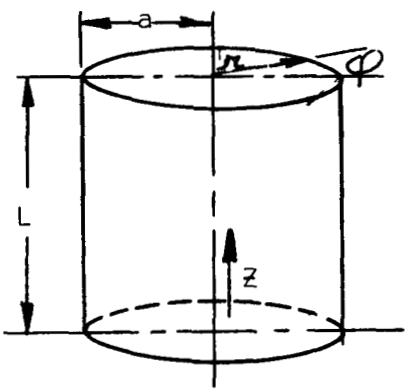

*All symbols used in the text are also defined under "NOMENCLATURE."

At the walls of the cylinder the particle velocity perpendicular to the wall must be zero. This means that the derivative of the pressure with respect to the coordinate perpendicular to the wall in question must be zero.

Considering the end wall, where the coordinate "z" is either zero or equal to "L", this requires that $\left.\frac{\partial p}{\partial z}\right|_{\substack{z=0 \\ z=L}}$ be zero. The partial derivative with respect to z is

$$\frac{\partial p}{\partial z} = \cos(m\varphi) J_m\left(\frac{\omega_r r}{c}\right) e^{-2\pi i \nu t}\left(-\frac{\omega_z}{c}\right) \sin\left(\frac{\omega_z z}{c}\right) \qquad (3)$$

which results from differentiating Equation (2). Equation (3) is identically zero when z is zero since the sine of zero is zero. For the derivative to be zero at $z = L$ the quantity $\frac{\omega_z L}{c}$ must be equal to $n_z \pi$ where n_z can assume any positive integral value.

Considering the r-direction for the radial particle velocity to be zero, $\frac{\partial p}{\partial r}$ must equal zero. Differentiating Equation (2) with respect to r,

$$\frac{\partial p}{\partial r} = \cos(m\varphi) \cos\left(\frac{\omega_z z}{c}\right) e^{-2\pi i \nu t} \frac{d}{dr}\left[J_m\left(\frac{\omega_r r}{c}\right)\right] \qquad (4)$$

For Equation (4) to be zero at $r = a$, the quantity dJ_m/dr must be zero at $r = a$, which will be true if $\omega_r a/c$ is equal to $\pi\alpha_{mn}$ where $\pi\alpha_{mn}$ is a solution to the equation $dJ_m(\pi\alpha)/d\alpha = 0$.

The boundary conditions determine the characteristics values to be inserted in the solution to the wave equation

$$\omega_z = (\pi n_z c/L) \quad \text{where } n_z = 0, 1, 2, 3, \ldots$$

$$\omega_r = (\pi \alpha_{mn} c/a)$$

$$\nu = \frac{c}{2}\sqrt{\left(\frac{n_z}{L}\right)^2 + \left(\frac{\alpha_{mn}}{a}\right)^2}$$

After inserting these values, Equation (2) becomes

$$p = \cos(m\varphi)\cos\left(\pi n_z \frac{z}{L}\right) J_m\left(\frac{\pi \alpha_{mn} r}{a}\right) e^{-c\pi i \sqrt{\left(\frac{n_z}{L}\right)^2 + \left(\frac{\alpha_{mn}}{a}\right)^2}\, t} \qquad (5)$$

Equation (5) is the general equation for standing waves in a closed cylindrical chamber. Although this is the general equation the pressure at any point can be thought of as the sum of the pressures due to several waves. The waves can be labeled "axial" or "tangential" depending upon their motion with respect to the chamber coordinates.

The z-axial or longitudinal waves have all the motion parallel to the chamber axis. The gas properties in any plane perpendicular to the axis are constant across the chamber. Under these conditions the quantity $\left[\cos(m\varphi)\right] J_m\left(\frac{\pi \alpha_{mn} r}{a}\right)$ must be zero for all values of φ and r which will be true only if "m" and "α_{mn}" are zero. With these substitutions Equation (5) becomes

$$p = \cos\left(\pi n_z \frac{z}{L}\right) e^{-c\pi i \frac{n_z}{L} t} \quad (n_z = 0, 1, 2, 3, \cdots) \qquad (6)$$

This type of resonance is the so-called "organ-pipe" mode since it is the dominant one for the large length-to-diameter ratios used in organ pipes.

However, for length-to-radius ratios less than 1.71 the mode with the lowest frequency $\left(\nu = \left[\left(n_z/L\right)^2 + \left(\frac{\alpha_{mn}}{a}\right)^2\right]^{1/2}\right)$ is a transverse "sloshing" mode. The motion in this "sloshing" or tangential mode is parallel to the curved side walls of the cylinder. There is no motion at the axis and gas properties are constant along any line parallel to the axis. The resulting equation for tangential modes is

$$p = \cos(m\varphi) J_m\left(\pi \alpha_{mo} \frac{r}{a}\right) e^{-c\pi i \frac{\alpha_{mo} t}{a}} \quad (m = 0, 1, 2, 3, \cdots) \qquad (7)$$

The waves in which all motion is parallel to the radii of the chamber are designated r-axial or radial waves. There is no variation with φ and z, and therefore "m" and "n" are zero. The expression for the pressure is then

$$p = J_0\left(\frac{\alpha_{on} r}{a}\right) e^{-c\pi i \frac{\alpha_{on}}{a} t} \qquad (n = 0, 1, 2, 3, \ldots) \tag{8}$$

Any standing wave pattern can be broken down into one or a combination of the preceding types of waves. Figure 1 on the following page shows some of the pressure patterns associated with these various modes.

B. Integrated Response of Transducers

Many of the transducers to be evaluated will have fairly large diaphragms as the sensing elements. Some simple assumptions as to the characteristics of these diaphragms are made in order to permit prediction of transducer response to the pressure patterns of the resonance modes of the cylindrical chamber. Some of the assumptions are

(1) The diaphragm forms one end wall of a closed cylinder which can be driven to resonance

(2) The output of the transducer is proportional to the instantaneous average pressure over the diaphragm

(3) The response of the diaphragm does not affect the standing wave patterns.

The known pressure patterns which will be considered first are those resulting from the standing waves present in a closed cylinder at resonance. Since it has been assumed that the modes can be superposed, each type of wave can be analyzed separately and the results added to obtain the net effect upon the diaphragm.

The solution for standing waves in a closed cylinder has

---NEGATIVE PRESSURE —— POSITIVE PRESSURE

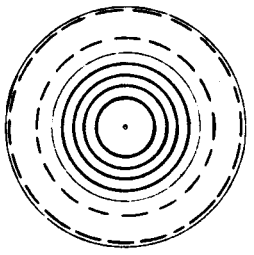

$\alpha_{01} = 1.2197$
FIRST RADIAL

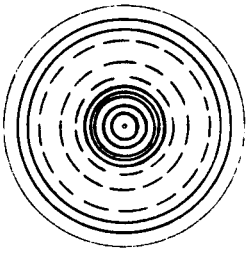

$\alpha_{02} = 2.2331$
SECOND RADIAL

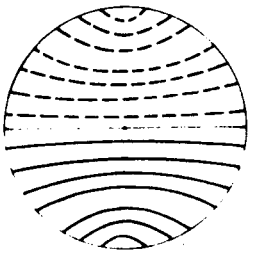

$\alpha_{10} = 0.5861$
FIRST TANGENTIAL

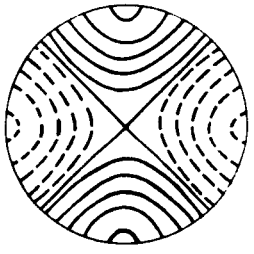

$\alpha_{20} = 0.9722$
SECOND TANGENTIAL

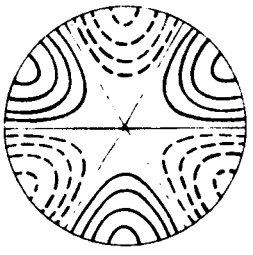

$\alpha_{30} = 1.3373$
THIRD TANGENTIAL

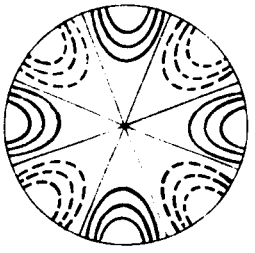

$\alpha_{40} = 1.6926$
FOURTH TANGENTIAL

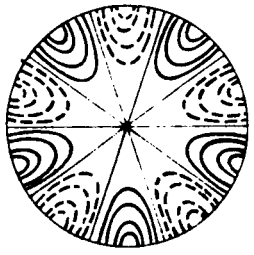

$\alpha_{50} = 2.0421$
FIFTH TANGENTIAL

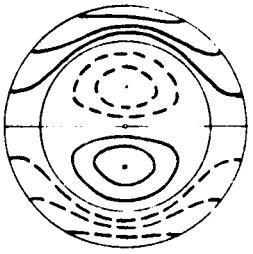

$\alpha_{11} = 1.6970$
FIRST COMBINED

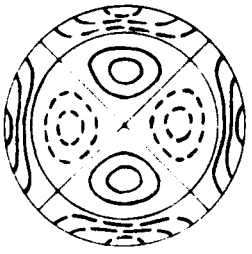

$\alpha_{21} = 2.1346$
SECOND COMBINED

TRANSVERSE MODES OF PRESSURE OSCILLATION
IN A CYLINDRICAL CHAMBER

JPR 1261

FIGURE 1

been developed previously and is

$$p = \cos(m\varphi)\cos\left(\pi n_z \frac{z}{L}\right) J_m\left(\frac{\pi \alpha_{mn} r}{a}\right) e^{-c\pi i\sqrt{\left(\frac{n_z}{L}\right)^2+\left(\frac{\alpha_{mn}}{a}\right)^2}\,t} \tag{9}$$

Consider first the response to longitudinal modes. It is evident that the average pressure over the diaphragm is in phase with and equal in amplitude to the pressure at the center of the diaphragm. The output of the transducer is then in phase with the pressure at the center of the diaphragm, and the amplitude is proportional to the amplitude at the center. For the purposes of this development the constant of proportionality may be assumed to be unity. The expression for the pressure at $z = L$ is

$$p = \cos(\pi n_z) e^{-c\pi i \frac{n_z}{L} t} \tag{10}$$

The average pressure over the area of the diaphragm from $r = 0$ to $r = r_1$ where $r_1 \leq a$ can be expressed as

$$p_a = \frac{\int_A p\,dA}{\int_A dA} = \frac{\int_0^{r_1}\int_0^{2\pi} p\,r\,d\varphi\,dr}{\int_0^{r_1}\int_0^{2\pi} r\,d\varphi\,dr} = \frac{\cos(\pi n_z) e^{-c\pi i \frac{n_z}{L} t}}{\pi r_1^2}\int_0^{r_1}\int_0^{2\pi} r\,d\varphi\,dr \tag{11}$$

R_1 is used to allow the actual or effective area to be less than the cross-sectional area of the chamber. Equation (11) neglects any non-varying component of the pressure. Evaluating the double integral the average pressure is

$$p_a = \cos(\pi n_z)\, e^{-c\pi i \frac{n_z}{L} t} \tag{12}$$

This is to be compared to the pressure at the center of the diaphragm. At the center, r is zero. The pressure at the center is then

$$p_c = \cos(\pi n_z)\, e^{-c\pi i \frac{n_z}{L} t} \tag{13}$$

This is identical in form with the expression for the average pressure. The diameter of the diaphragm thus has no effect upon the output

for longitudinal modes.

The situation is completely different when the tangential modes are considered. The expression for the average pressure when tangential modes are present is

$$p_a = \frac{1}{\pi r_1^2} \int_0^{r_1} \int_0^{2\pi} \cos(m\varphi)\, J_m\left(\frac{\pi \alpha_{mo} r}{a}\right) e^{-c\pi i \frac{\alpha_{mo} t}{a}} r\, dr\, d\varphi \quad (14)$$

This is obviously zero since the integral of a cosine function is zero when evaluated between the limits of zero and 2π radians.

The pressure at the center can be obtained by putting r equal to zero. The pressure at the center is

$$p_c = \cos(m\varphi)\, J_m(0)\, e^{-c\pi i \frac{\alpha_{mo}}{a} t} \quad (15)$$

and is zero because the Bessel functions J_m are zero for "m" greater than zero.

The transducer therefore should not respond to tangential modes.

For radial modes the pressure distribution is axisymmetric, and the pressure can be expressed as

$$p = J_0\left(\frac{\pi \alpha_{on} r}{a}\right) e^{-c\pi i \frac{\alpha_{on}}{a} t} \quad (16)$$

Defining average pressure as before, and substituting for "p" in the integral, the average pressure is given by the double integral

$$p_a = \frac{1}{\pi r_1^2} \int_0^{r} \int_0^{2\pi} J_0\left(\frac{\pi \alpha_{on} r}{a}\right) e^{-c\pi i \frac{\alpha_{on}}{a} t}\, r\, dr\, d\varphi \quad (17)$$

The quantity $e^{-c\pi i \frac{\alpha_{on}}{a} t}$ is not a function of either φ or r and can be taken outside the double integral. The average pressure is then

$$p_a = \frac{e^{-c\pi i \frac{\alpha_{on}}{a} t}}{\pi r_1^2} \int_0^{r_1} \int_0^{2\pi} J_0\left(\frac{\pi \alpha_{on} r}{a}\right) r\, dr\, d\varphi \quad (18)$$

The Bessel function $J_0(\frac{\pi\alpha_{on}r}{a})$ and r are not functions of ϕ and after integration with respect to ϕ the average pressure is

$$p_a = \frac{2e^{-c\pi i\frac{\alpha_{on}}{a}t}}{r_1^2}\int_0^{r_1} J_0\left(\frac{\pi\alpha_{on}r}{a}\right) r\,dr \qquad (19)$$

Change the running variable by letting $X = \frac{\pi\alpha_{on}r}{a}$

$$p_a = \left(\frac{2e^{-c\pi i\frac{\alpha_{on}}{a}t}}{r_1^2}\right)\left(\frac{a}{\pi\alpha_{on}}\right)^2\int_0^{X_1} X\,J_0(X)\,dX \qquad (20)$$

The integral $\int X J_0(X)dX$ is a standard form whose value is $X_1 J_1(X_1)$.

The average pressure is then

$$p_a = \left\{\left(\frac{2a}{r_1\pi\alpha_{on}}\right) J_1\left(\frac{\pi\alpha_{on}r_1}{a}\right)\right\} e^{-c\pi i\frac{\alpha_{on}}{a}t} = K e^{-c\pi i\frac{\alpha_{on}}{a}t} \qquad (21)$$

K is a constant dependent upon r_1 , a and α_{on}. For $r_1 = a$ the average pressure is zero, and there should not be any output from the transducer.

The pressure at the center of the end wall of the chamber is

$$p_c = J_0(0)\,e^{-c\pi i\frac{\alpha_{on}}{a}t} = e^{-c\pi i\frac{\alpha_{on}}{a}t} \qquad (22)$$

The average pressure and the pressure at the center are in phase but the amplitude ratio is dependent upon the constant K . In all cases, however, the average pressure is less than or equal to the pressure at the center.

The preceding discussion considered the response of a transducer to the pressure patterns present in a cylinder at resonance. The theory will now be extended to a somewhat more general case, that of a sinusoidal pressure wave moving parallel to the diaphragm of the transducer.

Assume that the transducer is mounted flush in the walls of a rocket motor and is exposed to tangential resonance modes. It is necessary

to determine the errors in phase and amplitude caused by the area of the circular diaphragm.

The following assumptions are made:

1. The sensing element of the transducer is a flat circular diaphragm of radius R .
2. The pressure can be represented as a steady pressure plus a sinusoidal component which moves parallel to a diameter of the diaphragm.
3. The steady pressure can be ignored.
4. The net deflection of the diaphragm is proportional to the instantaneous average pressure over the diaphragm.

From assumption 1. the pressure can be represented as

$$p = p_M + A\cos 2\pi f(t+t_o) \tag{23}$$

The diaphragm can be represented as a circular area in the x-y coordinate plane bounded by the curve $x^2 + y^2 = R^2$.

In terms of the coordinate x the pressure at any point can be represented as

$$p_x = p_M + A\cos 2\pi f\left(\frac{x}{c}+\frac{x_o}{c}\right) = p_M + A\cos\left[\left(\frac{2\pi f}{c}\right)x+\phi\right] \tag{24}$$

where the variable t has been replaced by an equivalent variable $\frac{x}{c}$. The expression $\phi = \frac{2\pi f}{c} x_o$ is essentially a phase angle which relates the position of the pressure wave with respect to the diaphragm. The mathematical model is presented below.

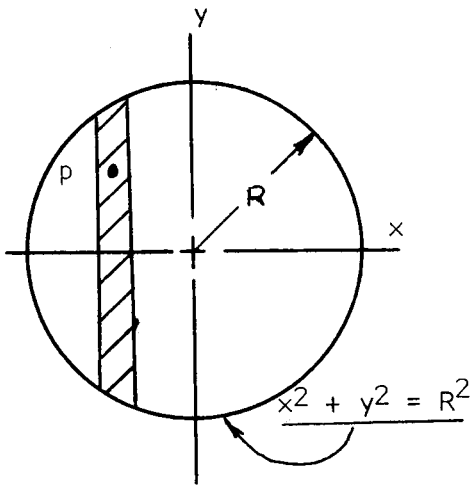

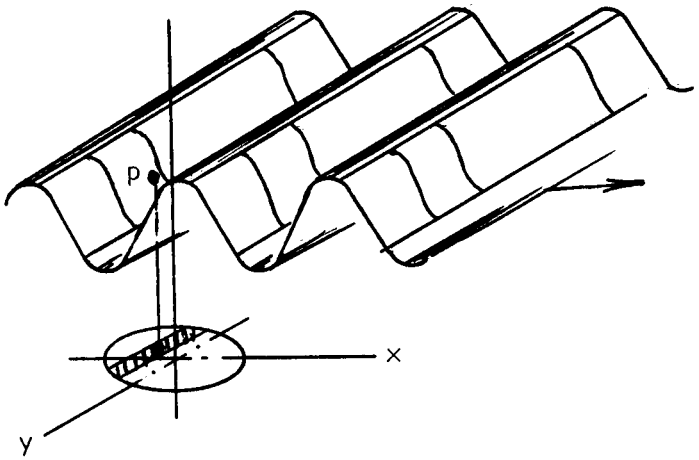

From this the instantaneous average pressure over the diaphragm is

$$\bar{p} = \frac{\int_A p\,dA}{\int_A dA} = \frac{4\int_0^R \left[p_M + A\cos\left\{\left(\frac{2\pi f}{c}\right)x + \phi\right\}\right]\sqrt{R^2-x^2}\,dx}{4\int_0^R \sqrt{R^2-x^2}\,dx} \tag{25}$$

The response of the diaphragm will be compared to the pressure at the center as a reference. At the center $x = 0$ and

$$\bar{p} = p_M + A\cos\phi \tag{26}$$

Rearranging Equation (25) the average pressure can be represented as

$$\bar{p} = p_M \frac{4\int_0^R \sqrt{R^2-x^2}\,dx}{4\int_0^R \sqrt{R^2-x^2}\,dx} + \frac{4\int_0^R \left[A\cos\left\{\left(\frac{2\pi f}{c}\right)x + \phi\right\}\right]\sqrt{R^2-x^2}}{4\int_0^R \sqrt{R^2-x^2}\,dx} \tag{27}$$

or

$$\bar{p} = p_M + \frac{\int_0^R \left[A\cos\left\{\left(\frac{2\pi f}{c}\right)x + \phi\right\}\right]\sqrt{R^2-x^2}\,dx}{\int_0^R \sqrt{R^2-x^2}\,dx}$$

Change the running variable and make the following substitutions

$$w = x/R$$
$$K = 2\pi f R/c$$

Then

$$\bar{p} = p_M + \frac{4A}{\pi}\int_0^1 \sqrt{1-w^2}\,\cos(kw+\phi)\,dw \tag{28}$$

The integral $\int_0^1 \sqrt{1-w^2}\cos(kw+\phi)\,dw$ has been integrated numerically for values of K from zero to five and values of ϕ from zero to two radians. After normalizing by dividing by $\int_0^1 \sqrt{1-w^2}\,dw = \frac{\pi}{4}$ the results are plotted for comparison with $p = \cos\phi$ for ϕ from zero to two radians in Figure 2. There is a phase shift and amplitude decrement dependent upon R and K where $K = \frac{2\pi f}{c}$. For a diaphragm of radius $R = 0.35"$, a wave propagation velocity $c = 3500$ ft/sec and a frequency of 1600 cps the phase shift would be approximately 25 degrees

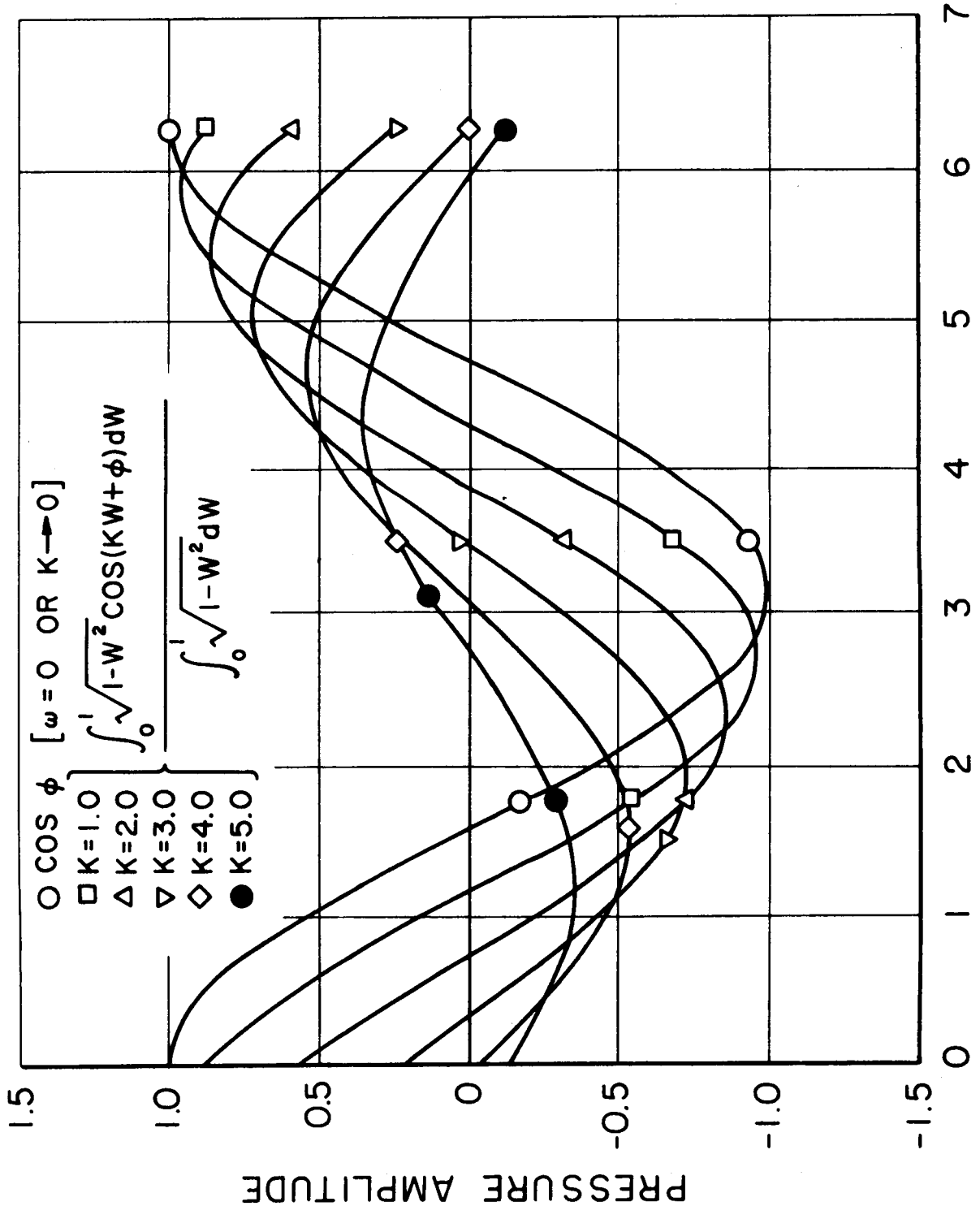

INTEGRATED TRANSDUCER RESPONSE TO A PARALLEL INCIDENT SINUSOIDAL WAVE

FIGURE 2

and the amplitude ratio would be 0.88.

This effect should therefore be considered when using transducers where the pressure pattern is moving parallel to the sensing element diaphragm.

IV. EXPERIMENTAL STUDY

A. Apparatus

The test chamber of the pressure generator was a small cylinder 0.70 inches in diameter and 0.255 inches in length. During transducer evaluation the test transducer and its mounting formed one end wall of the chamber. The chamber was designed around the Dynisco PT49 series of pressure transducers, and this dictated the minimum possible chamber diameter and also the chamber configuration; i.e., a cylinder rather than a sphere or a cube. A reference pickup with a very high resonant frequency was mounted in the opposite end wall.

The gas whose flow was to be modulated entered through an orifice 1/10" in diameter in the curved side wall of the chamber and discharged through a circular port 1/8" in diameter across the chamber from the inlet port.

An aluminum wheel having seventy-two 1/8" diameter circular holes near its rim rotated past the discharge port, thereby modulating the flow. The wheel could be adjusted against the chamber block by a micrometer adjustment.

A detailed drawing of the Sinusoidal Pressure Generator is presented in Figure 3.

The drive used for these tests was a U.S. Varidrive with an output speed range of 1500-6000 rpm. The drive from the Varidrive to the modulating wheel was through timing belts and gears. Two gear ratios, 1:1 and 3:1 were used to provide a speed range of 1500-18,000 rpm for the wheel. Photographs of the generator system are presented in Figures 4 and 5.

When using the generator for routine transducer evaluation the chamber response should be as nearly sinusoidal in waveform as possible. In order to satisfy this requirement, the lowest resonant chamber frequency

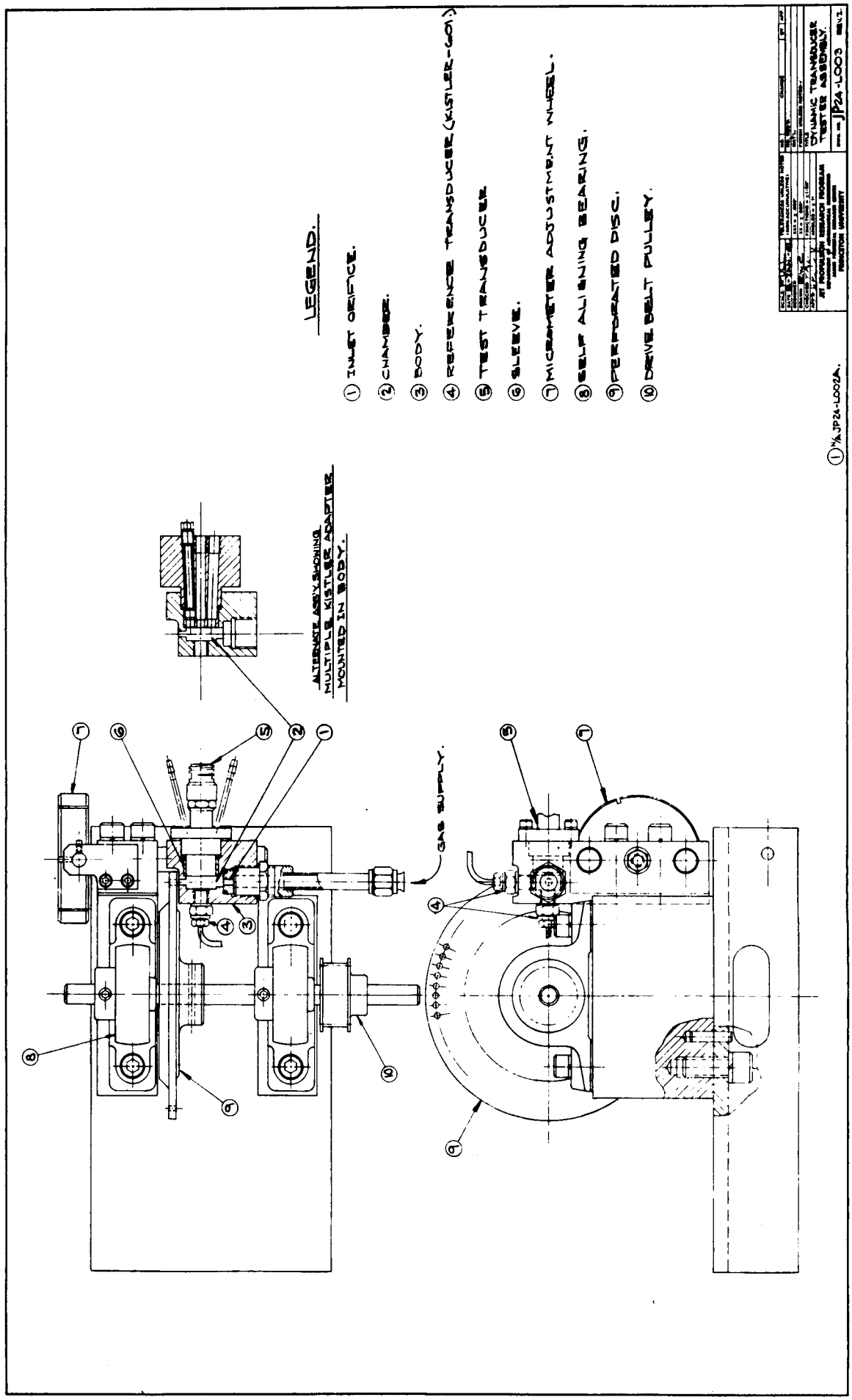

FIGURE 3

SINUSOIDAL PRESSURE GENERATOR

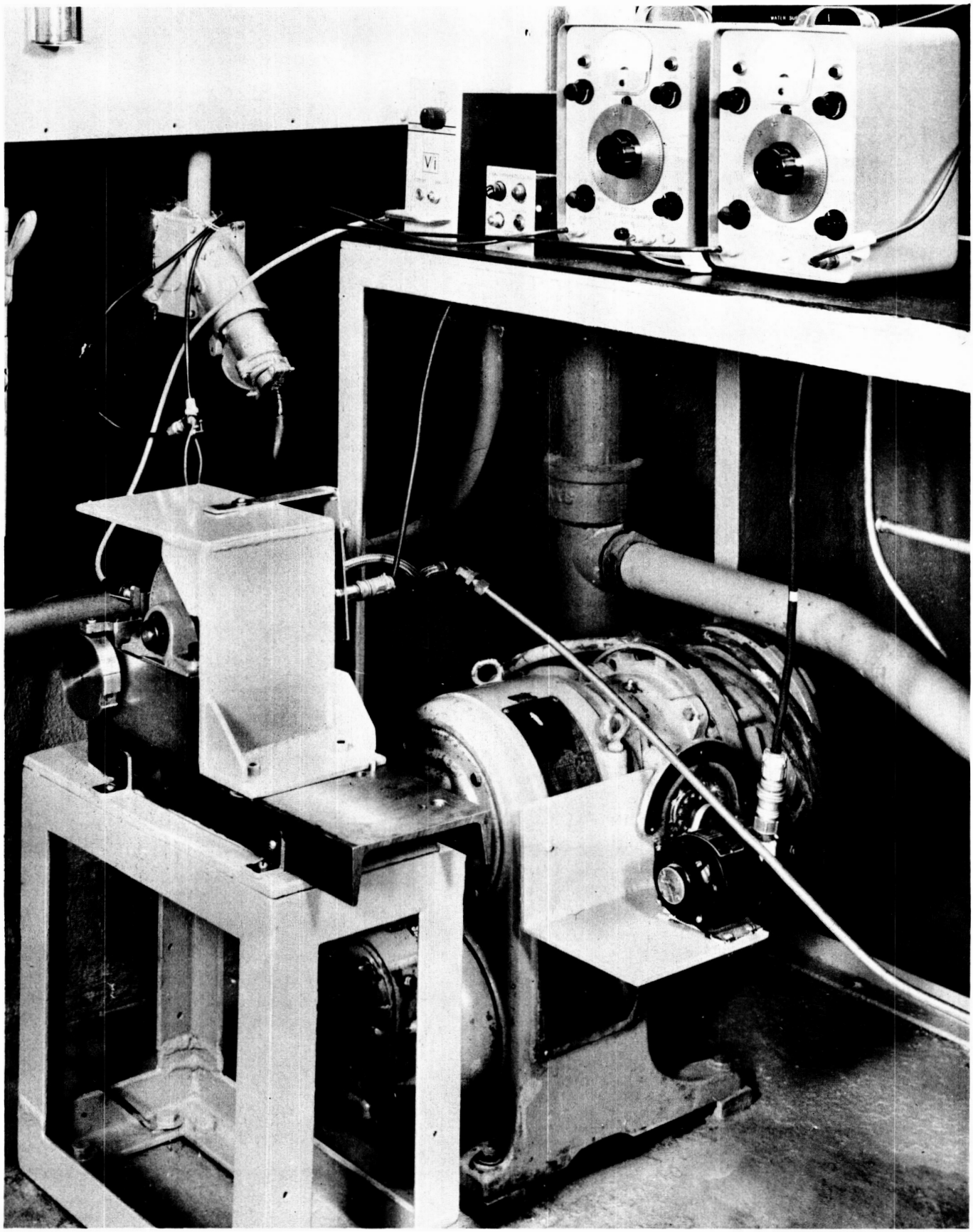

SINUSOIDAL PRESSURE GENERATOR
AND INSTRUMENTATION

FIGURE 4

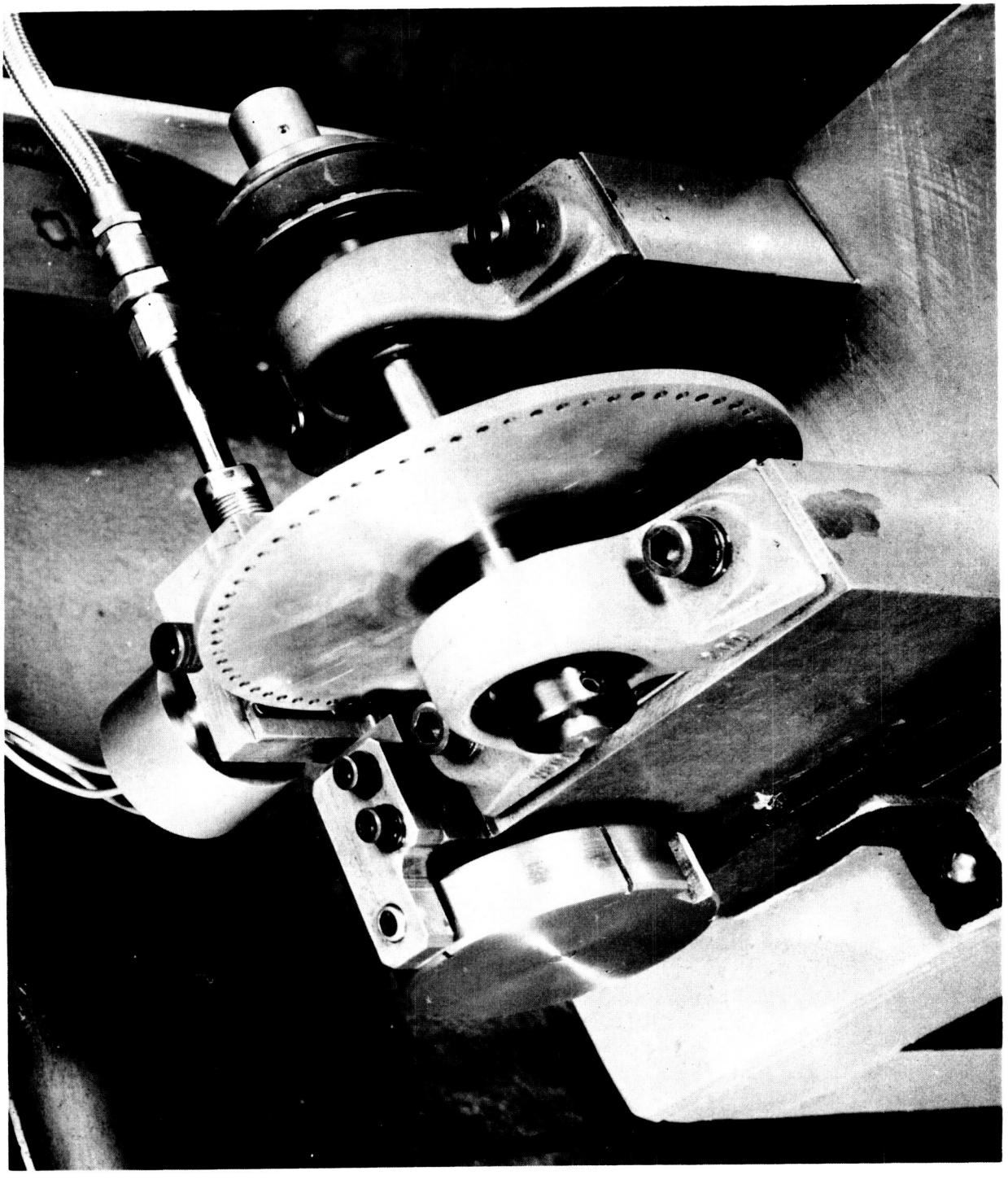

SINUSOIDAL PRESSURE GENERATOR

FIGURE 5

should be as high as possible. The ideal gas for this reason would have been hydrogen, but it was rejected because of the hazards associated with its use in a confined area. Helium, being inert, was chosen for transducer evaluation.

In order to study the response of the chamber, some of the theoretical chamber resonances must be within the possible riving frequency range of 1800-21,600 cps. Since the resonantfrequencies are directly proportional to the speed of wave propagation, it was decided to use nitrogen and Freon-12, which have rather low propagation velocities (of the order of 1100 ft/sec and 500 ft/sec respectively at room temperature).

The helium was stored in a compressed gas bottle. From the bottle the helium passed through two stages of pressure regulation. Supply pressure into the generator was arbitrarily set at 90 psig. Flow to the generator was controlled by a remotely-operated solenoid valve.

The nitrogen system was similar to the helium system except that the nitrogen was drawn directly from a high-pressure nitrogen cascade.

The Freon-12 was supplied from a bottle heated by resistance heating cables and went through only one pressure regulator. There was effectively no pressure regulation, since the maximum Freon-12 pressure attained, approximately 80 psig, was below the regulated pressure of 90 psig.

The gas systems are presented in Figure 6.

The three transducers used for evaluation of the pressure generator were piezo-electric quartz transducers which had a resonant frequency of approximately 127,000 cps (shock tube determination). The active sensing surface of these pickups was less than a tenth of an inch in

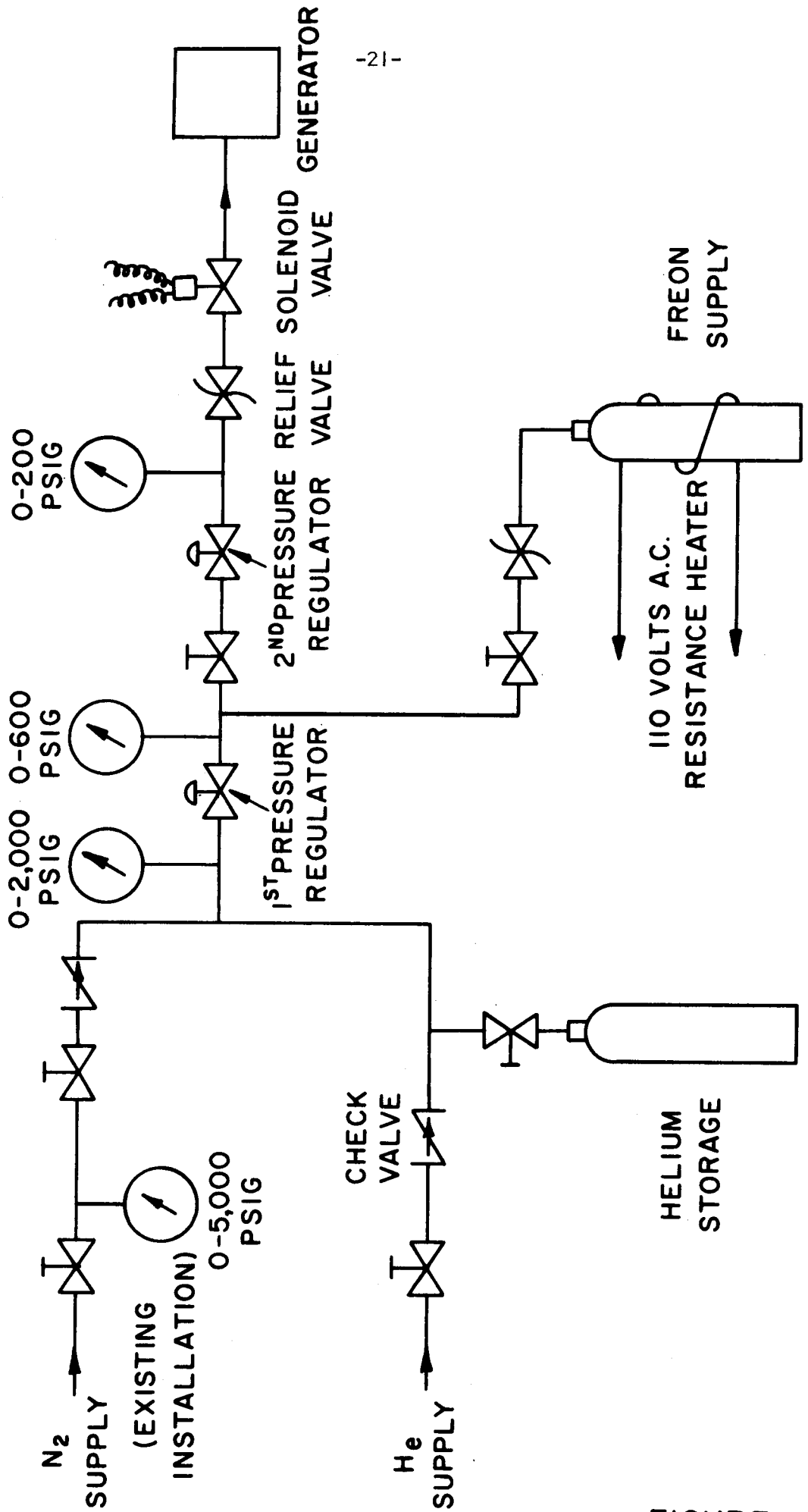

GAS SUPPLY SYSTEMS

FIGURE 6

JPR 1264

diameter. Although only the varying component of the chamber pressure was measured, these pickups exhibited good D.C. stability when used carefully. Their output was of the order of one volt, which was amplified through an amplifier-calibrator having a maximum gain of six. Because the resonant frequency of the quartz transducers was high, it was assumed that their output faithfully reproduced the actual chamber response. A transducer with a resonant frequency of 127,000 cps and fairly high damping would have, at 20,000 cps, a phase lag of approximately ten degrees and an amplitude ratio very nearly equal to one. Using the transducer outputs directly was thus sufficiently accurate within the frequency range of the generator.

The only "test" transducer used was one of the Dynisco PT49 series, which utilized bonded strain gages and employ double diaphragms for water cooling. These tranducers have an approximate resonant frequency of 25,000 cps and low damping. A regulated power supply was used for excitation of the test transducer and the signal was amplified through a D.C. amplifier operated differentially.

From the amplifiers the signals were fed through filters and then into the amplifying units of a four channel oscilloscope. The filters were designed primarily to eliminate high frequency noise and any possible resonant response of the quartz transducers. The circuit diagram of these filters and their amplitude and phase characteristics are discussed in Appendix B.

The oscilloscope has a four-beam cathode ray tube. The four beams have common triggering and sweep circuits; however, there are two controls, each controlling two beams, for horizontal trace positioning. For this reason marker pulses were placed on all traces simultaneously

for more accurate determination of phase relationships.

Driving frequency was calculated from wheel speed. A small two pole magnet was mounted on the wheel shaft and a small coil was mounted near the magnet. The frequency generated as the shaft turned was displayed on an electronic counter.

All waveforms were photographed using a Polaroid camera mounted on the oscilloscope.

The instrumentation schematic appears in Figure 7. The two types of transducers used are shown in Figure 8 along with the quartz transducer adapter, the chamber inlet orifice, and the Dynisco transducer adapter ring. The four-channel oscilloscope, Polaroid camera, filters, and marker amplifier are shown in Figure 9.

B. Tests

With the transducers installed and the test gas flowing, the sinusoidal pressure generator was operated over a range of speeds and the chamber response photographed from the oscilloscope display.

For the chamber evaluation a special plug was designed to hold as many as four of the quartz transducers. The plug was inserted in the same location that a test transducer would occupy during evaluation. This arrangment provided information on the chamber response at five different locations on the chamber end wall. A drawing of this plug is presented in Figure 10, and an exploded view of the entire pickup-plug assembly is presented in Figure 11. This special plug was used for all of the tests except those for determination of the integrated response of a test transducer to known pressure patterns.

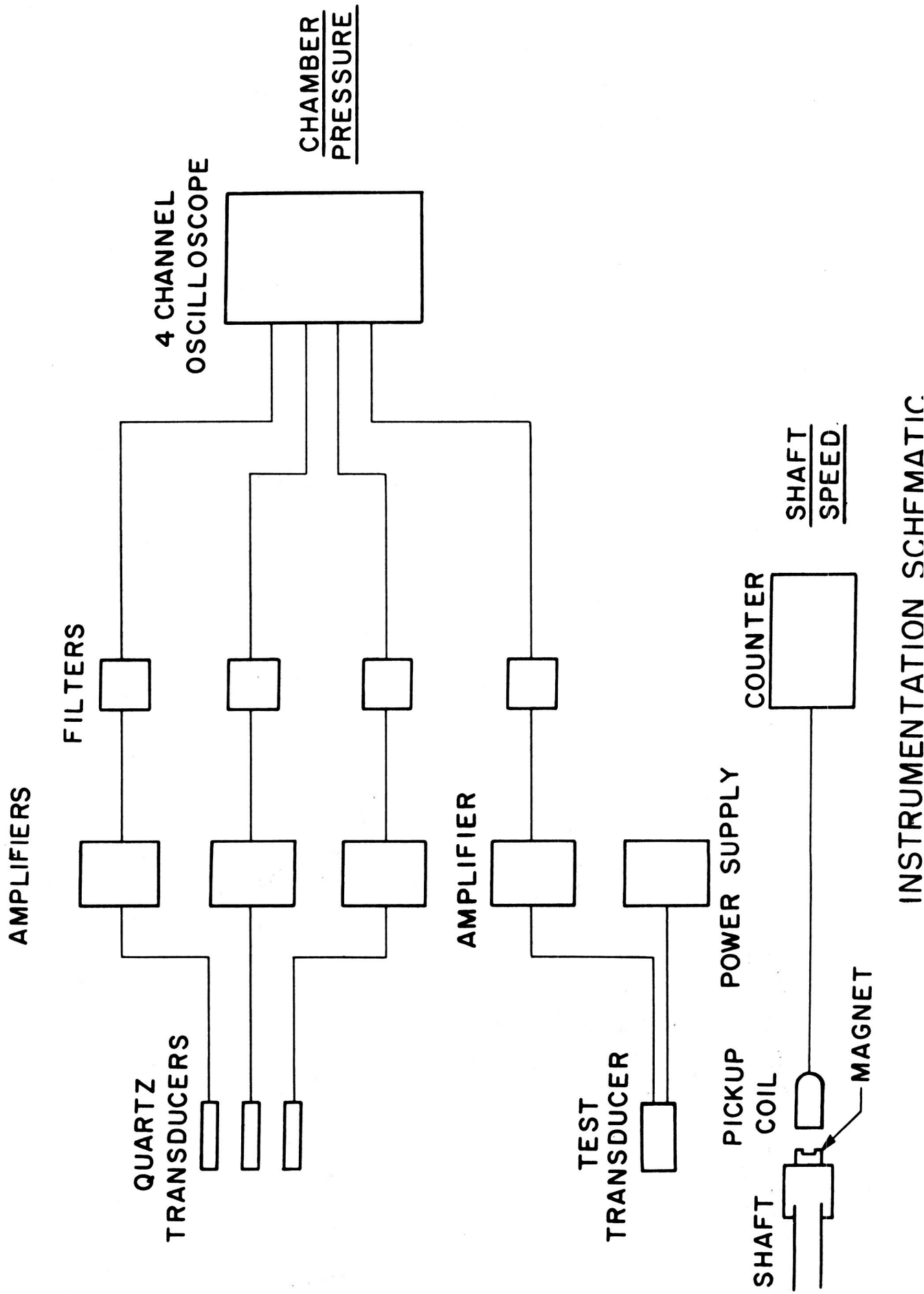

FIGURE 7 INSTRUMENTATION SCHEMATIC

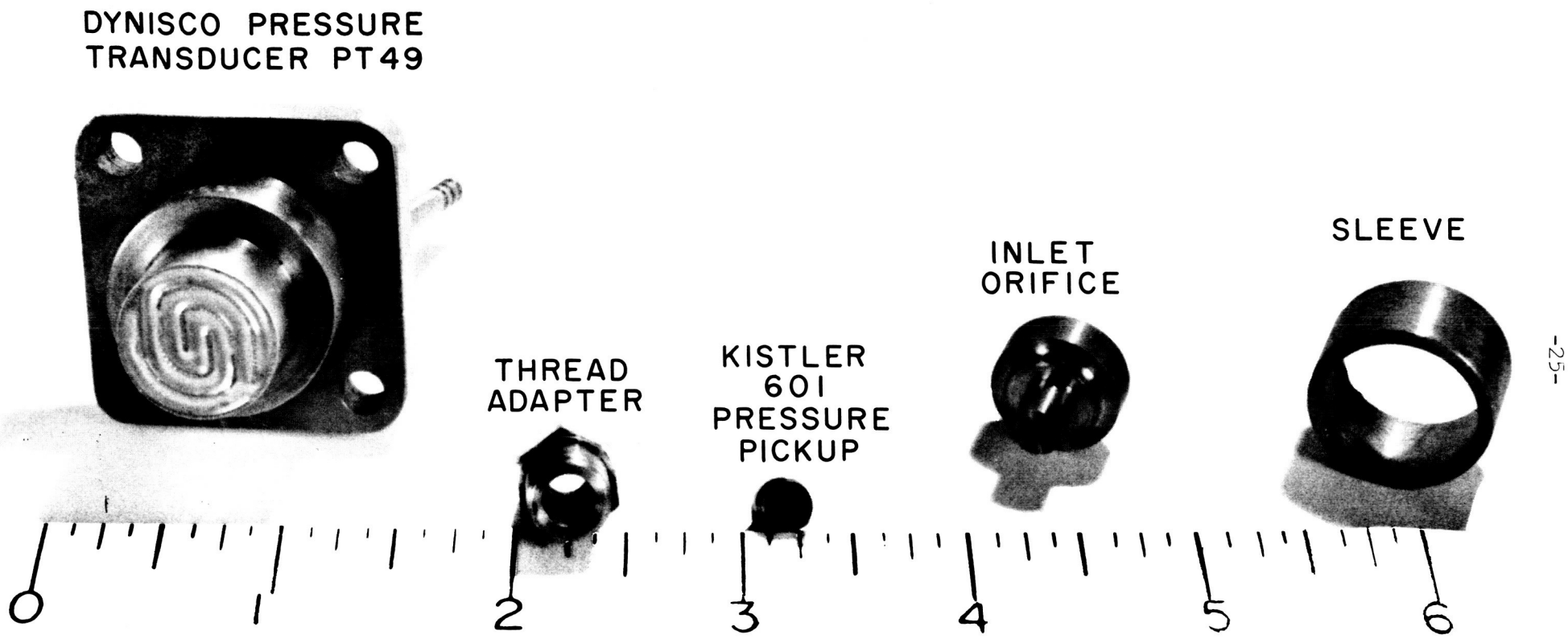

FIGURE 8

PRESSURE TRANSDUCERS, INLET ORIFICE, AND PICKUP ADAPTER RING

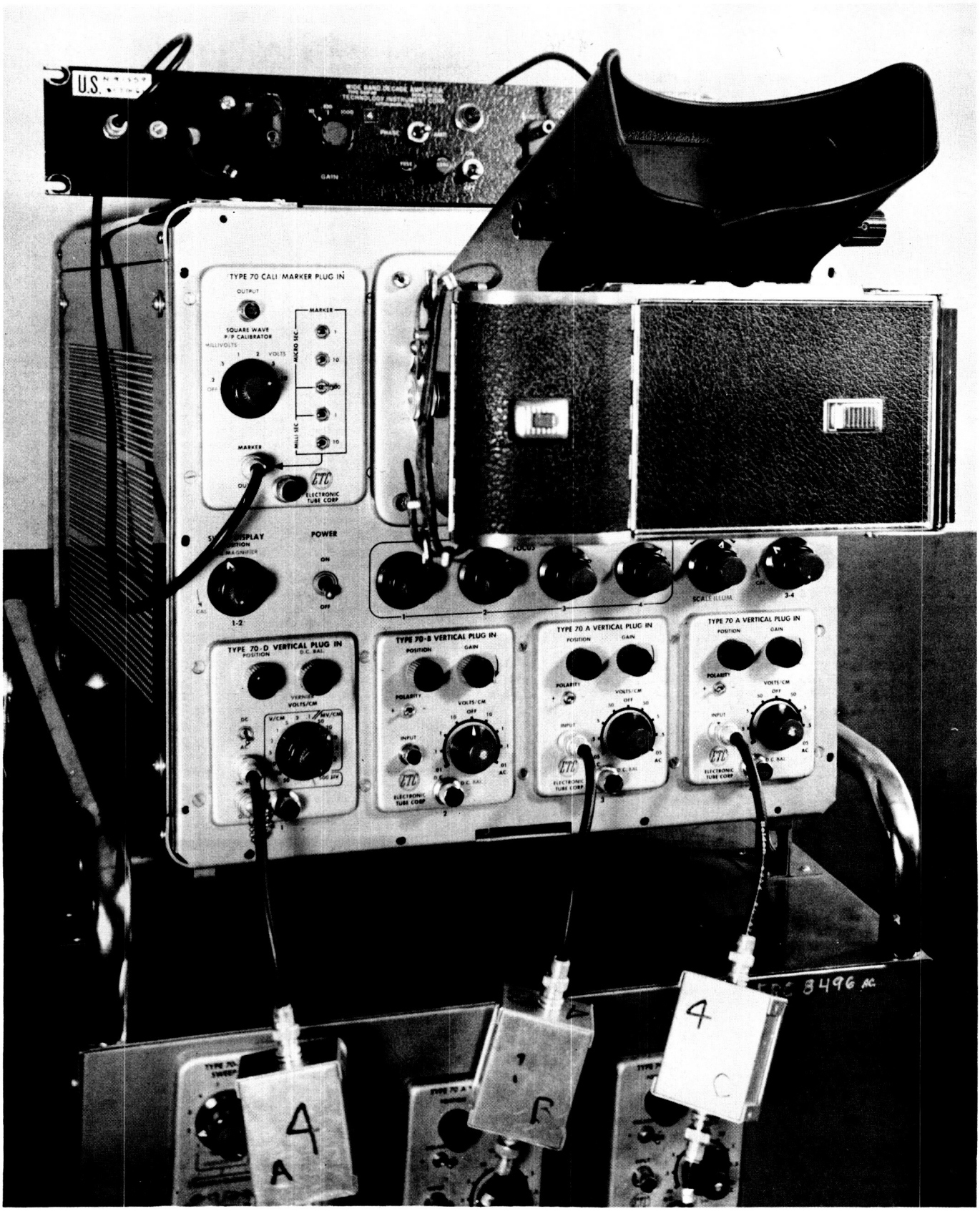

FOUR BEAM OSCILLOSCOPE WITH CAMERA AND FILTERS

FIGURE 9

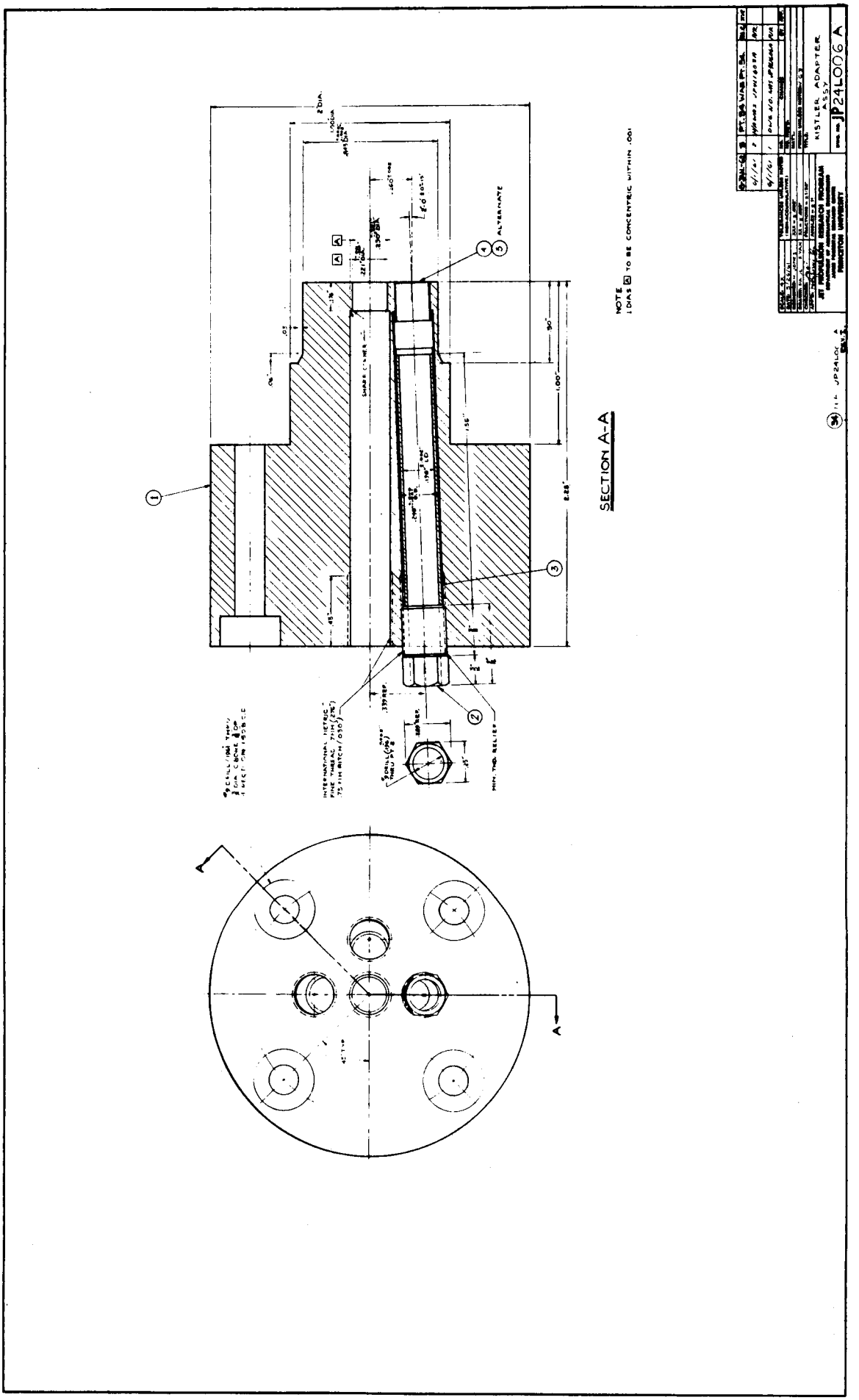

TRANSDUCER ADAPTER ASSEMBLY

FIGURE 10

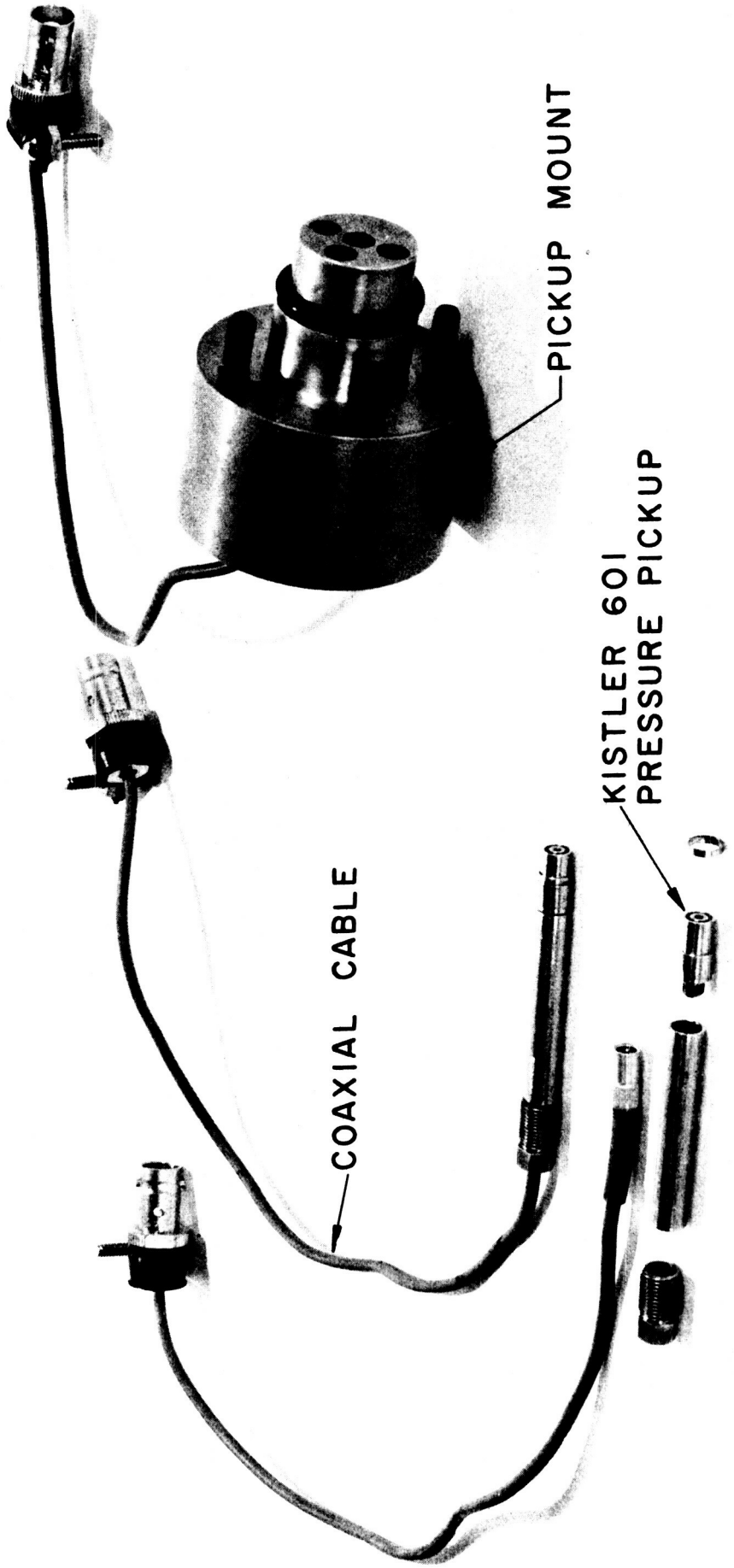

EXPLODED VIEW OF TRANSDUCER ADAPTER ASSEMBLY

FIGURE 11

The following diagram shows one typical configuration for the location of the transducers in relation to the chamber:

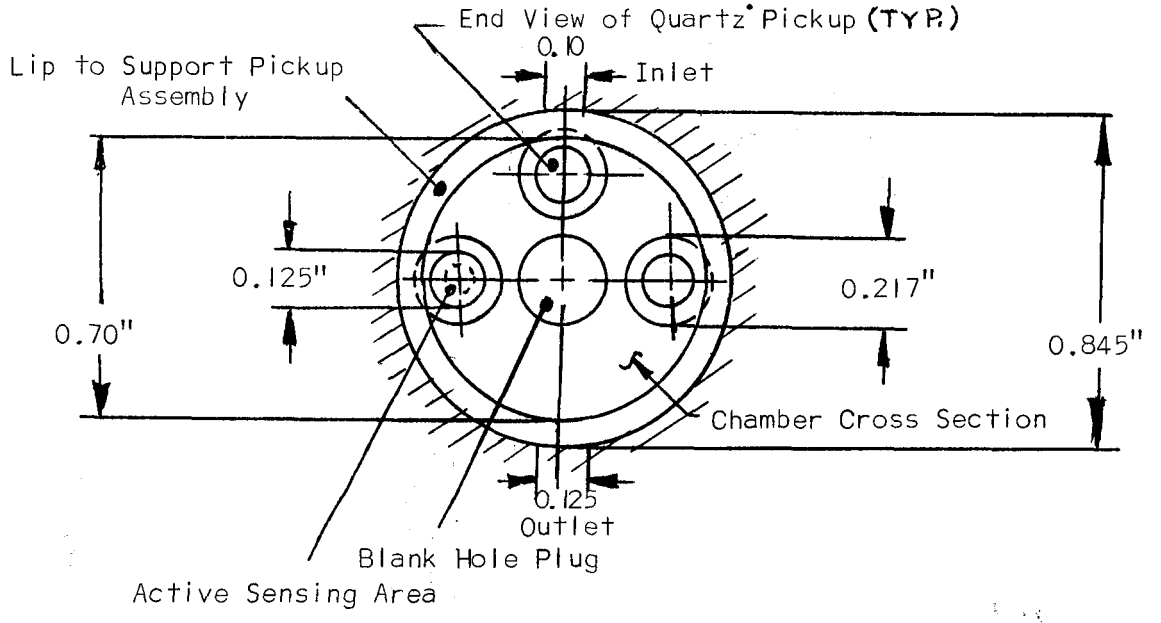

C. Problems and Discussion of Errors

Electromagnetic Interference

The most serious problem was 60 cycle interference, particularly with the strain-gage transducer, because of the very high gain necessary to obtain adequate signal amplitude. The interference was reduced to a resonable level by a careful elimination of all ground loops and by operating the D.C. amplifier differentially.

This problem was not serious for the quartz transducers because of their relatively large outputs.

Frequency Errors

One obvious source of error was the accuracy of the electronic counter. The quoted accuracy was one count but the gating was such that it was possible to lose or gain almost two counts (two cycles). The driving

frequency was seventy-two times the count because there were seventy-two holes in the modulating wheel. At a driving frequency of 2000 cps the error could have been as much as 7.2 percent and at 20,000 cps the possible error was .72 percent.

Another problem which became serious after completion of these particular tests was inconstancy of the output speed of the Varidrive. This became progressively worse and was estimated to be several percent at the time the Varidrive was replaced by a direct-current motor.

Departure from a Sinusoidal Waveform

The response at off-resonance conditions should be sinusoidal for transducer evaluation, but an examination of the actual waveforms showed a departure from this ideal. The waveforms with helium were very nearly sinusoidal at the lower frequencies, but steepened as the frequency was increased. As the frequency was increased further, so that the wavelength was of the order of the chamber dimensions, the waveforms became quite distorted and the response was non-uniform across the chamber. There were several reasons for this behavior:

1. The aluminum modulating wheel used for these tests warped, producing a runout of .0015". This wheel wobble and the irregular gas leakage introduced frequencies other than the driving frequency.

2. The circular discharge holes did not theoretically produce the correct area variation for sinusoidal waveforms.

3. The turbulence level of the flow through the chamber could have been an appreciable fraction of the total output at the higher frequencies.

4. Flow intertia effects could have been responsible for the steepening of the waves but this was not investigated.

V. ANALYTICAL-EXPERIMENTAL CORRELATION

A. Response at Off-Resonance Conditions

The generator had adequate off-resonance response only with helium, which is the usual test gas for transducer evaluation. The mean chamber pressure was essentially constant with frequency, as can be seen from Figure 12. The mean pressure was 55.5 psig, as determined from the test transducer output display on a D.C. millivoltmeter.

The peak-to-peak amplitude of the fluctuating component of the pressure at various locations in the chamber is presented in Figure 13. The amplitude attenuated rapidly with frequency. The amplitude was obtained with an electronic voltmeter, which responded to the average voltage output of the quartz transducers.

The resulting pressure patterns as a function of the frequency are presented in Figures 14 and 15. The middle trace was not out of phase, as it would appear from the photographs, as can be seen by observing the location of the marker intervals on each trace. At the lower frequencies the response was very nearly sinusoidal and in phase. As the frequency of operation was increased the amplitude decreased and the waves tended to steepen. All the traces were obtained at constant gain settings so that the relative amplitudes are correct. As the amplitude decreased, the noise, turbulence, vibration, etc. became a larger fraction of the total output. At the highest frequencies the response became more irregular as discussed earlier, and phase relationships became difficult to determine.

It is desirable for transducer evaluation that the chamber response be uniform and sinusoidal. This criterion limited the existing test configuration to about 10,000 cps.

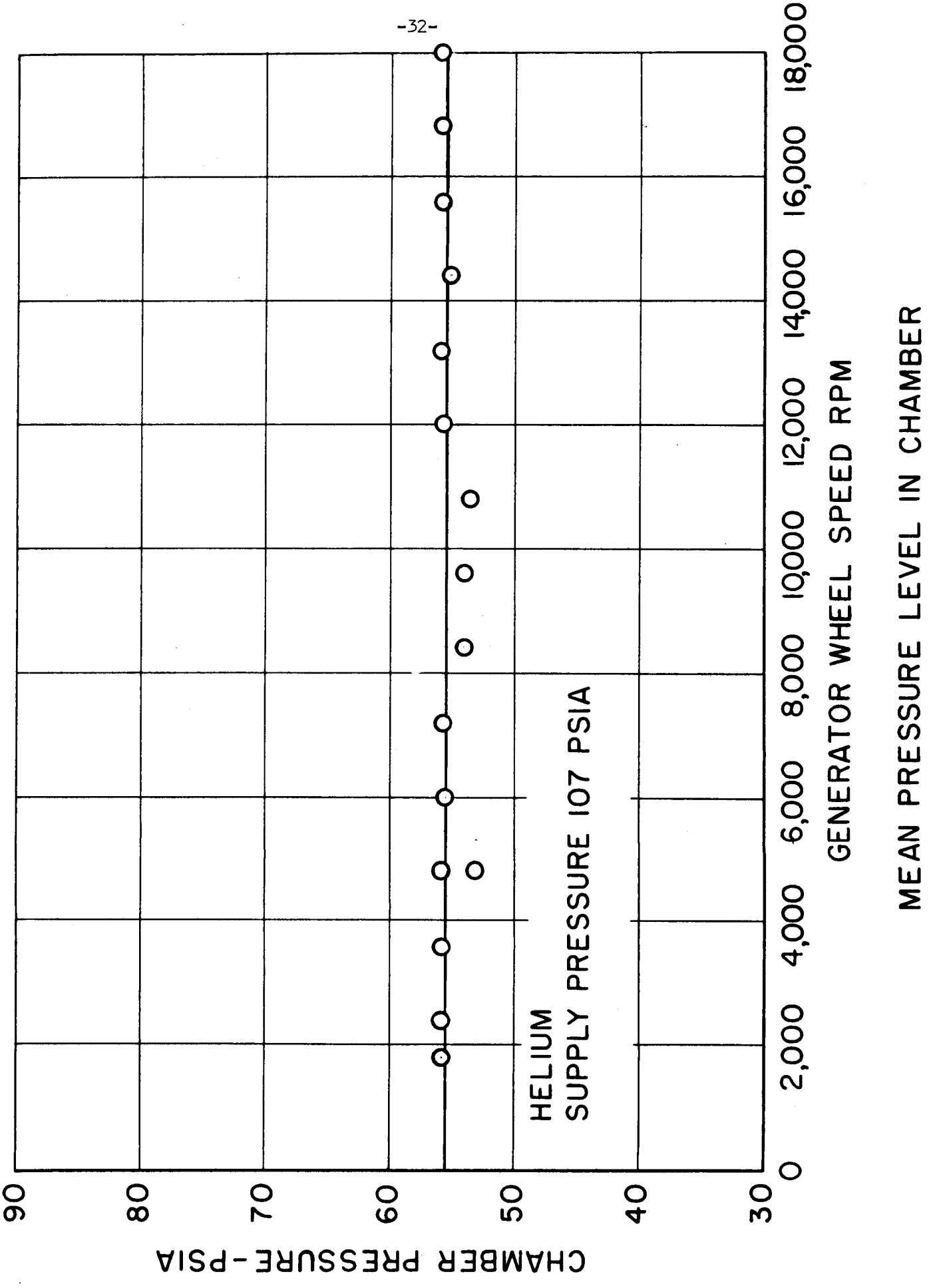

JPR 1266

FIGURE 12

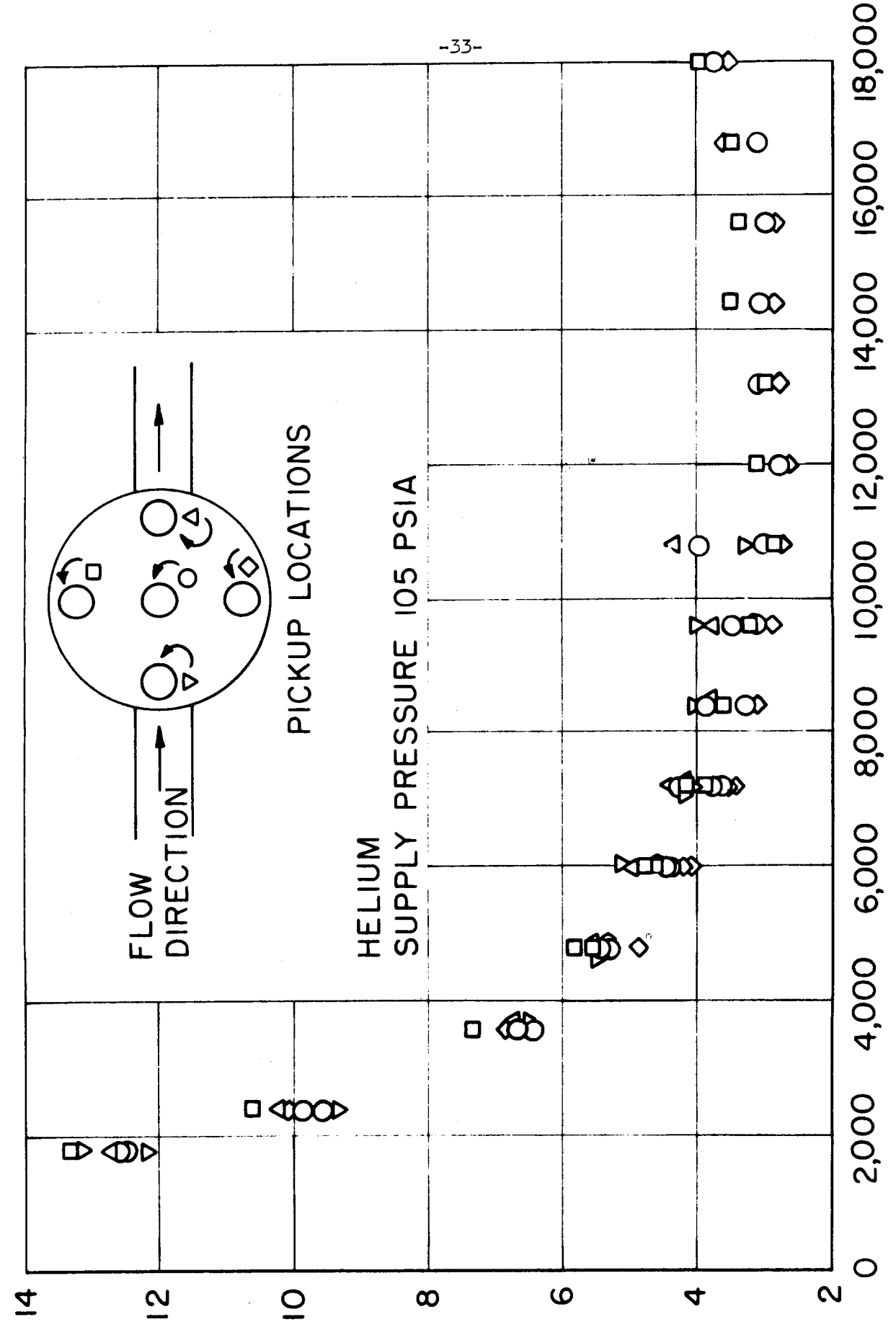
MAGNITUDE OF PRESSURE FLUCTUATIONS
GENERATOR WHEEL SPEED RPM
0
2,000
4,000
6,000
8,000
10,000
12,000
14,000
16,000
18,000
PRESSURE FLUCTUATIONS - PEAK TO PEAK PSI
2
4
6
8
10
12
14
HELIUM SUPPLY PRESSURE 105 PSIA
PICKUP LOCATIONS
FLOW DIRECTION

FIGURE 13

T-TOP TRACE M-MIDDLE TRACE B-BOTTOM TRACE

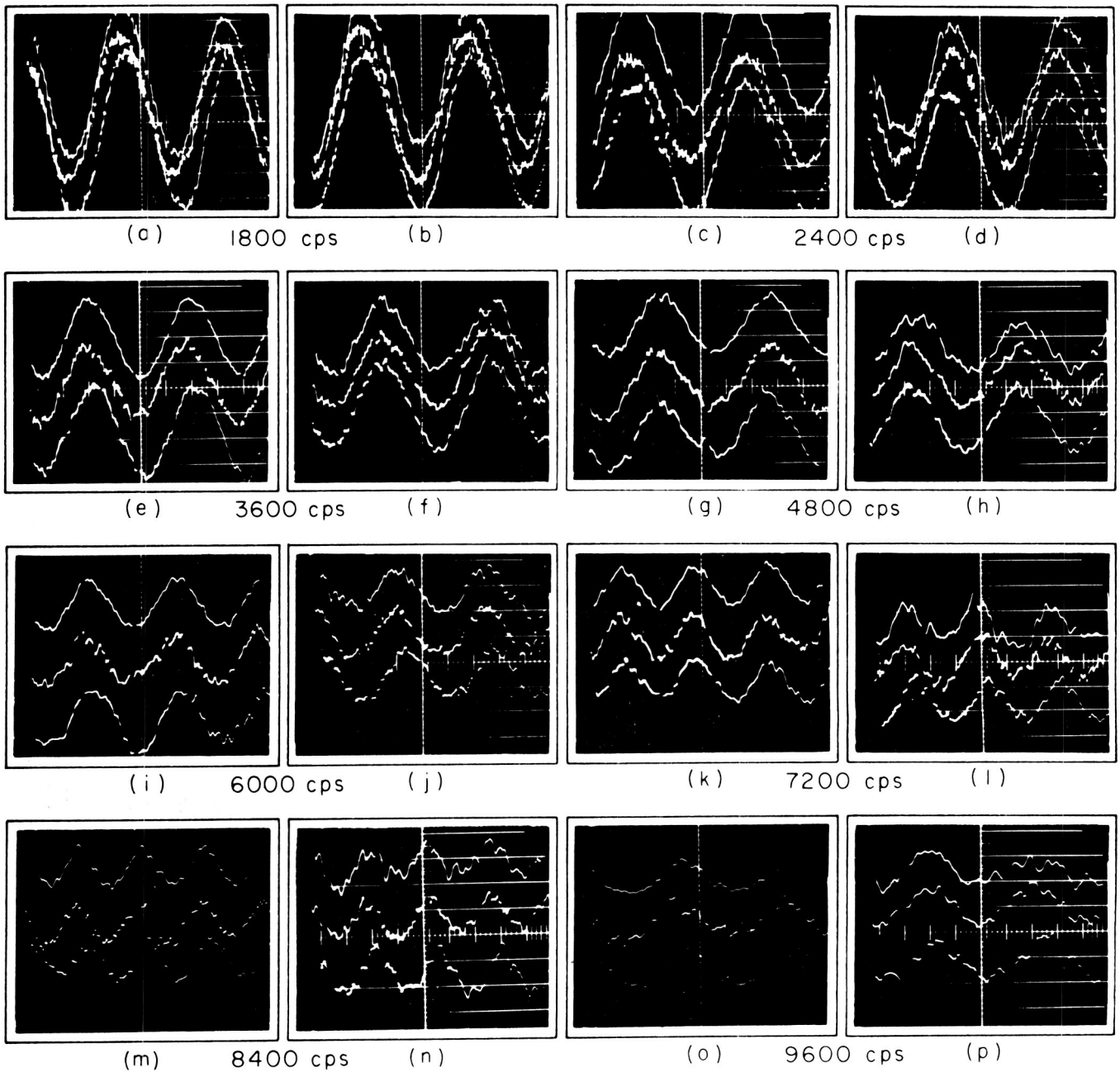

CHAMBER RESPONSE WITH HELIUM

FIGURE 14

T - TOP TRACE M - MIDDLE TRACE B - BOTTOM TRACE

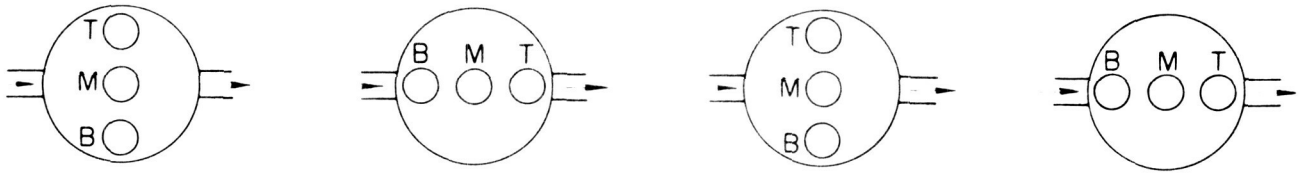

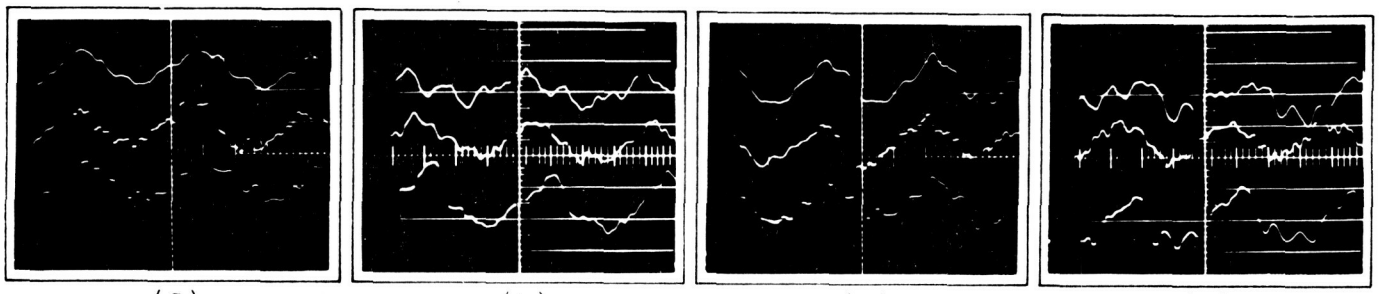

(a) 10800 cps (b) (c) 12000 cps (d)

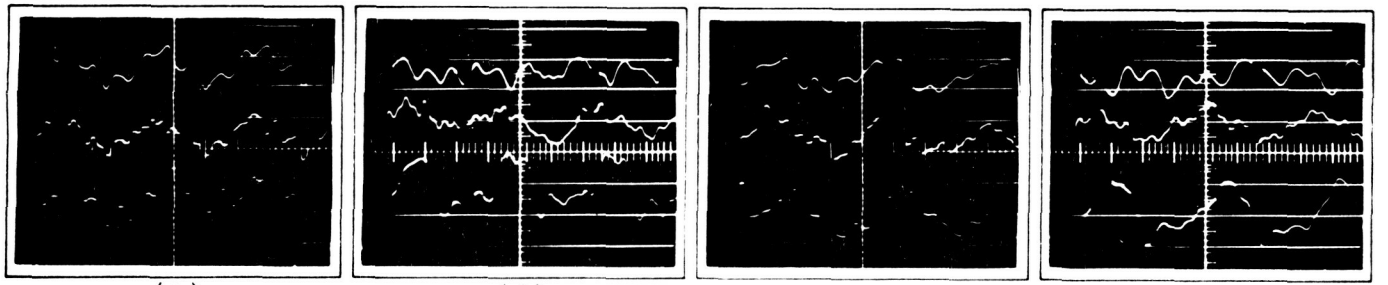

(e) 13200 cps (f) (g) 14400 cps (h)

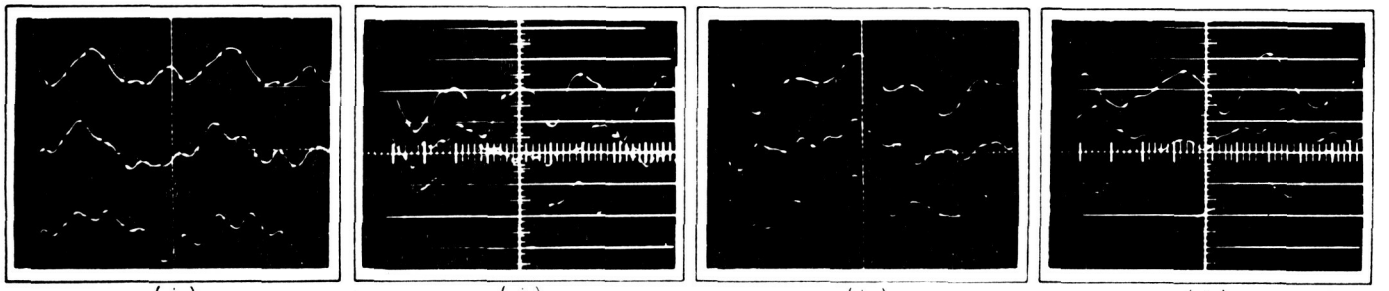

(i) 15600 cps (j) (k) 16800 cps (l)

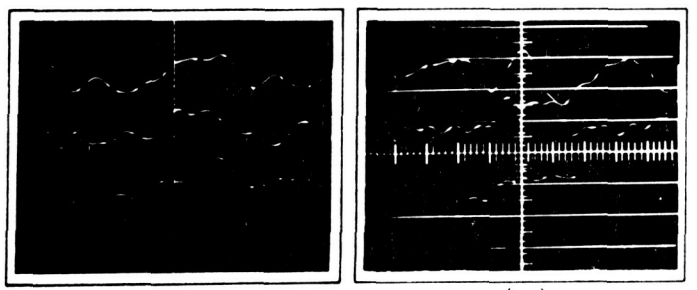

(m) 18000 cps (n)

CHAMBER RESPONSE WITH HELIUM

FIGURE 15

B. Chamber Resonance

Section III-A explored theoretically the standing wave patterns in a cylindrical chamber at resonance. In this section the existence of the resonance modes is experimentally demonstrated.

The radius, a , of the chamber was 0.35" and the length, L, was approximately 0.255". The latter dimension varied somewhat because the plug which formed the end wall had an "O" ring seal, and the dimension could vary depending upon the amount of compression of this seal.

The equations for the resonant frequencies of the various modes contain the velocity of wave propagation, c . It was assumed that the propagation velocity of the standing waves was equal to the propagation velocity of an infinitesimal pulse. The propagation velocity was then determined from the following equation:

$$c = \sqrt{\gamma g R T} \tag{29}$$

where R = gas constant $= R_o/M_o$

R_o = universal gas constant = 1545.4 ft lbf/lbm-mole ^{o}R

M_o = molecular weight

g = conversion factor = 32.17 ft/sec^2

γ = ratio of the specific heats

T = absolute temperature of the gas in degrees Rankine

The gas properties are listed in the following table.

Gas	Molecular Weight M_o	Ratio of the Specific Heats
Helium	4.003 (at. wt.)	1.67
Nitrogen	28.016	1.405
Freon-12	120.92	1.138

The temperature of the gases in the modulator chamber was determined experimentally by inserting a bare-junction thermocouple into the chamber through the sidewall transducer mounting hole. The gas temperatures were 67°F for Freon-12 and 72°F for nitrogen and helium.

The calculated propagation velocities were

$$c_{Helium} = 3321 \text{ ft/sec.}$$

$$c_{Nitrogen} = 1151 \text{ ft/sec.}$$

$$c_{Freon-12} = 496 \text{ ft/sec.}$$

These propagation velocities were used to calculate the resonant frequencies for the various modes. The calculated resonant frequencies are listed in the following table. These frequencies were calculated using $\nu = \frac{c}{2}\left[\left(\frac{n_z}{L}\right)^2 + \left(\frac{\alpha_{mn}}{a}\right)^2\right]^{1/2}$.

Resonant Frequencies

Pattern	m	n	n_z	Resonant Frequencies, Cps Freon-12	Nitrogen	Helium
1st Tangential	1	0	0	4,980	11,560	33,370
2nd Tangential	2	0	0	8,270	19,180	
1st Radial	0	1	0	10,380	24,070	69,440
1st Longitudinal	0	0	1	11,230	26,060	75,190
3rd Tangential	3	0	0	11,380		
Comb. 1st Tangential and 1st Longitudinal	1	0	1	12,320		
Comb. 2nd Tangential and 1st Longitudinal	2	0	1	13,950		
4th Tangential	4	0	0	14,400		
Comb. 1st Tangential and 1st Radial	1	1	0	14,420		
Comb. 1st Radial and 1st Longitudinal	0	1	1	15,320		
Comb. 3rd Tangential and 1st Longitudinal	3	0	1	16,000		
5th Tangential	5	0	0	17,380		
Comb. 2nd Tangential and 1st Radial	2	1	0	18,100		
Comb. 1st Longitudinal and 4th Radial	0	4	1	18,300		
2nd Radial	0	2	0	18,950		
6th Tangential	6	0	0	20,300		

The lowest resonant frequency with helium (33,370 cps) was above the driving frequency capability of the generator, and no clear-cut resonance pattern appeared. This section therefore considers only the Freon-12 and nitrogen results.

The three quartz transducers were mounted in the brass plug, and the remaining hole filled by using a blank plug made for this purpose. The pickups were placed either across a diameter or at 90° to each other around the edge of the chamber.

After a shutdown for an extended period, the amplitudes as indicated by the three transducers were adjusted so that all were equal when flowing helium at about 4000 cps. At this frequency the amplitude of the chamber response was still high and the waveform nearly sinusoidal. No special effort was made to maintain the amplitudes of the oscilloscope display constant from adjustment to adjustment, so that the apparent amplitudes vary somewhat between sets of runs.

1. Nitrogen

With nitrogen there were only two resonant chamber frequencies within the driving frequency range of 1800-21,600 cps: the first tangential mode, 11, 560 cps, and the second tangential mode, 19,180 cps.

Figure 16 presents all the results using nitrogen. The response between 1800 and 10,800 cps was repetitive but very distorted as compared to a sine wave. At 10,800 cps (16a, b, c) the pressure pattern was the stabilized first tangential mode; i.e., the responses near the inlet and discharge ports were of high amplitude and 180 out of phase with each other, at location 90° to the inlet and discharge ports the response was of low amplitude and more distorted, while the center was a null position.

At 11,280 cps (16d) the amplitude of the response was higher but

T - TOP TRACE M - MIDDLE TRACE B - BOTTOM TRACE

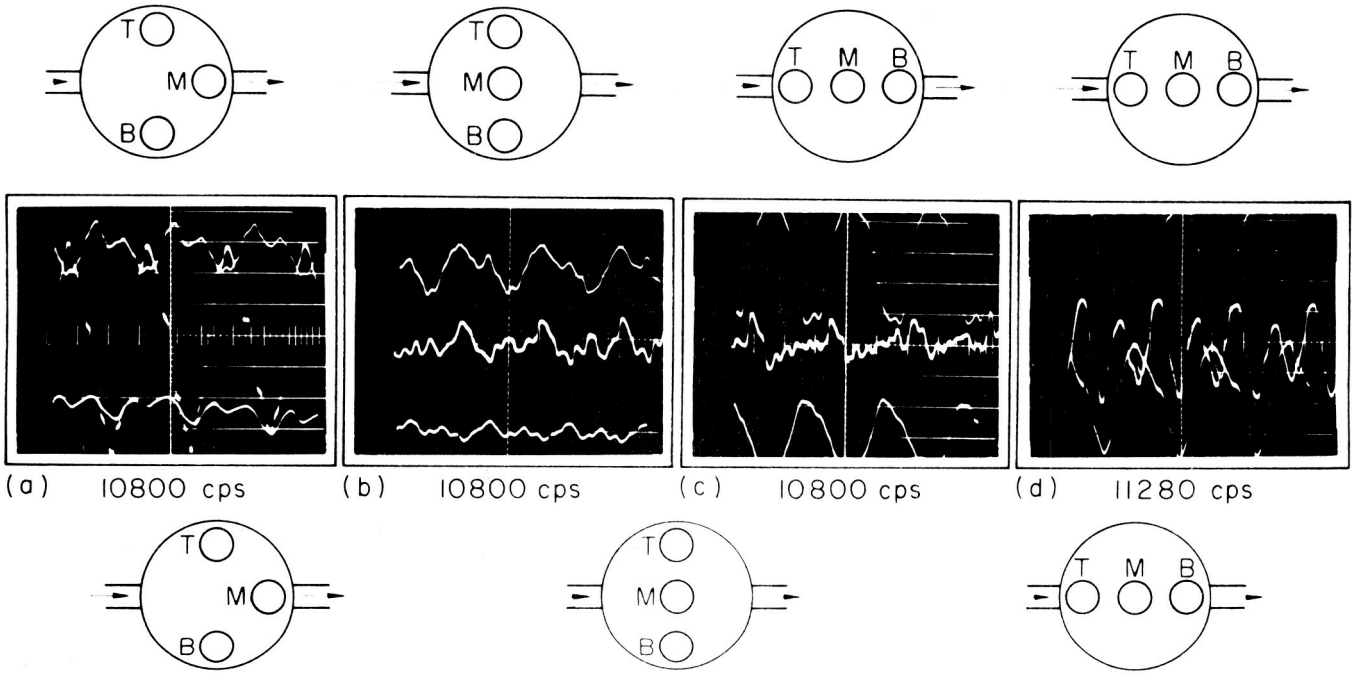

CHAMBER RESPONSE WITH NITROGEN

FIGURE 16

the center was affected more strongly than previously. The pattern was still basically the first tangential mode. Above 11,280 cps up to about 16,800 cps the response became more irregular and the amplitude decreased. The basic first tangential mode was apparent from about 9600 to 14,640 cps. The calculated resonant frequency (11,560 cps) was about midway in this range, but the best wave pattern occurred at a somewhat lower frequency.

For the stabilized second tangential mode the responses at locations diametrically opposite across the chamber should be in phase and the center should be a null. The behavior at 16,800 cps (16 e, f, g) indicated a second tangential mode; however, two of the photographs show a stabilized form (16f, g) and the third (16e), where the transducers were located around the edge, indicated a "spinning" form, since although the three traces had equal pressure amplitudes, the phase relationships were incorrect for a stabilized mode. This was the only instance in which a spinning mode was identifiable as such. From Maslen and Moore (4) the spinning mode is usually dominant over the standing mode unless the geometry dictates otherwise. In the modulator the flow of gas appeared to stabilize the mode with the nodes at 90° to a line joining the inlet and discharge ports.

At 18,000 cps where the three transducers were also located 90° apart (16h), the pattern was clearly a stabilized second tangential mode. All the results at 18,000 cps (16h) indicated the stabilized mode.

The pattern was still present at 19,200 cps (16k, l, m). This compares with the calculated resonant frequency of 19,180 cps.

The existence of the first and second tangential modes was therefore demonstrated experimentally by these tests. An unexpected development was the persistence of the basic pattern over a wide frequency range.

2. Freon-12

Within the frequency range of the generator there were many more resonances possible with Freon-12 than with nitrogen. From Reardon (5), for length-to-diameter ratios much less than unity, purely transverse modes should appear. In this case L/D = .382, which indicated that transverse modes should at least dominate. The most commonly observed modes, in order of increasing frequency, were the first tangential, the second tangential, the first radial, and the first combined radial-tangential.

Freon-12 results are presented in Figures 17, 18, and 19. The calculated resonant frequency of the first tangential mode was 4980 cps. Experimentally the resonant pattern appeared at about 4032 cps (17a,b) with the amplitude reaching a maximum at 4608 cps (17c, d, e). The basic pattern, although very distorted, was still present at 4944 cps (17f).

The second tangential mode was present from 6696 cps (17g) to about 7992 cps (17k, l). There were no records obtained of the response between 7992 and 9360 cps, so that it was impossible to determine if the pattern existed at the calculated resonant frequency of 8270 cps; however, the best pattern was obtained at 7300 cps, which was considerably less than the calculated value.

The first and second tangential modes were therefore definitely identified in both the nitrogen and Freon-12 tests, but the best patterns were obtained at frequencies less than the calculated resonant frequencies. With nitrogen the differences were small, on the order of several percent. With Freon-12 the differences were approximately ten percent. It was impossible to account completely for these differences, but several possible explanations are discussed below.

The calculation of the velocity of propagation could have been in error because of errors in the measurement of the temperature of the

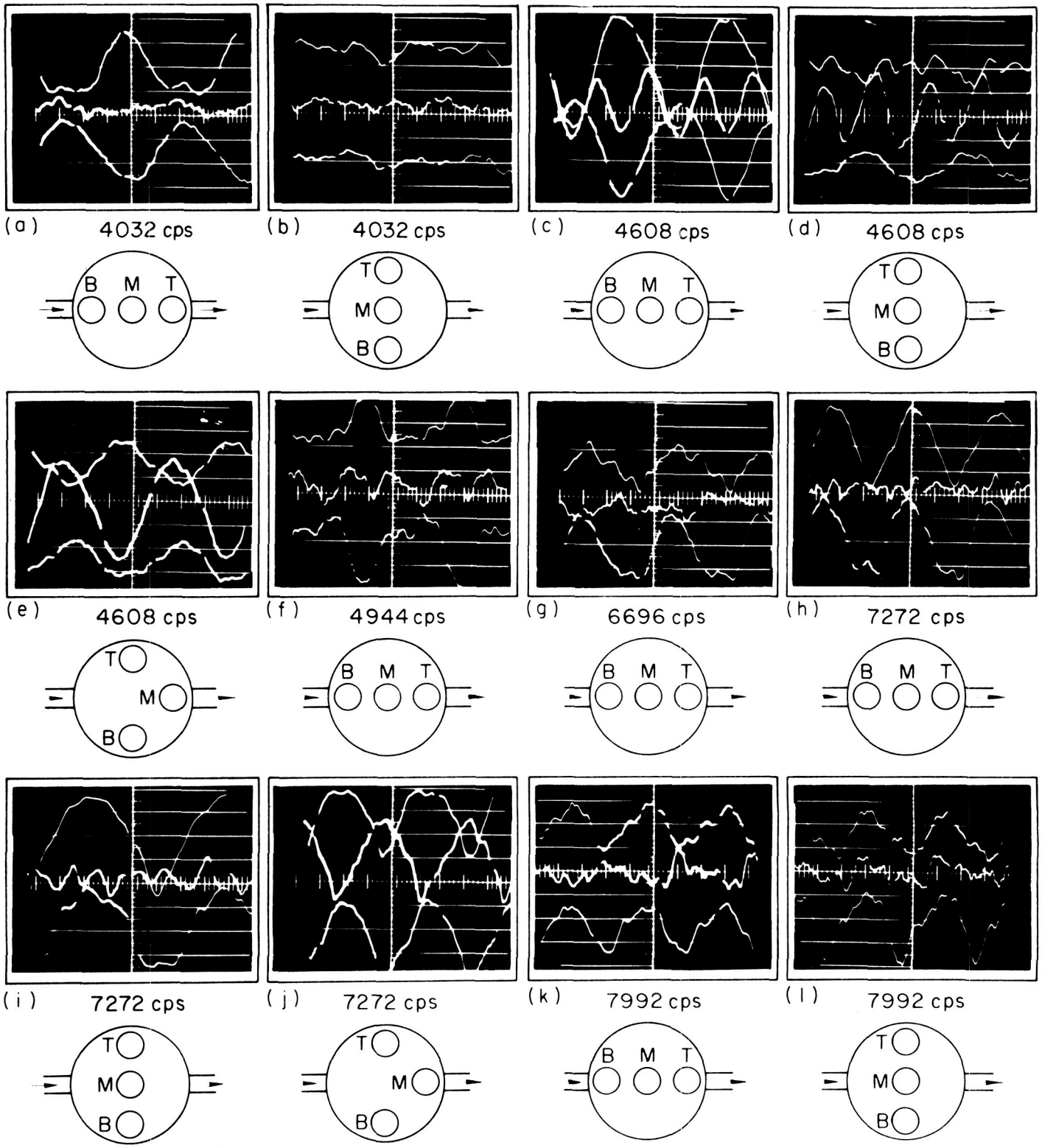

CHAMBER RESPONSE WITH FREON-12

FIGURE 17

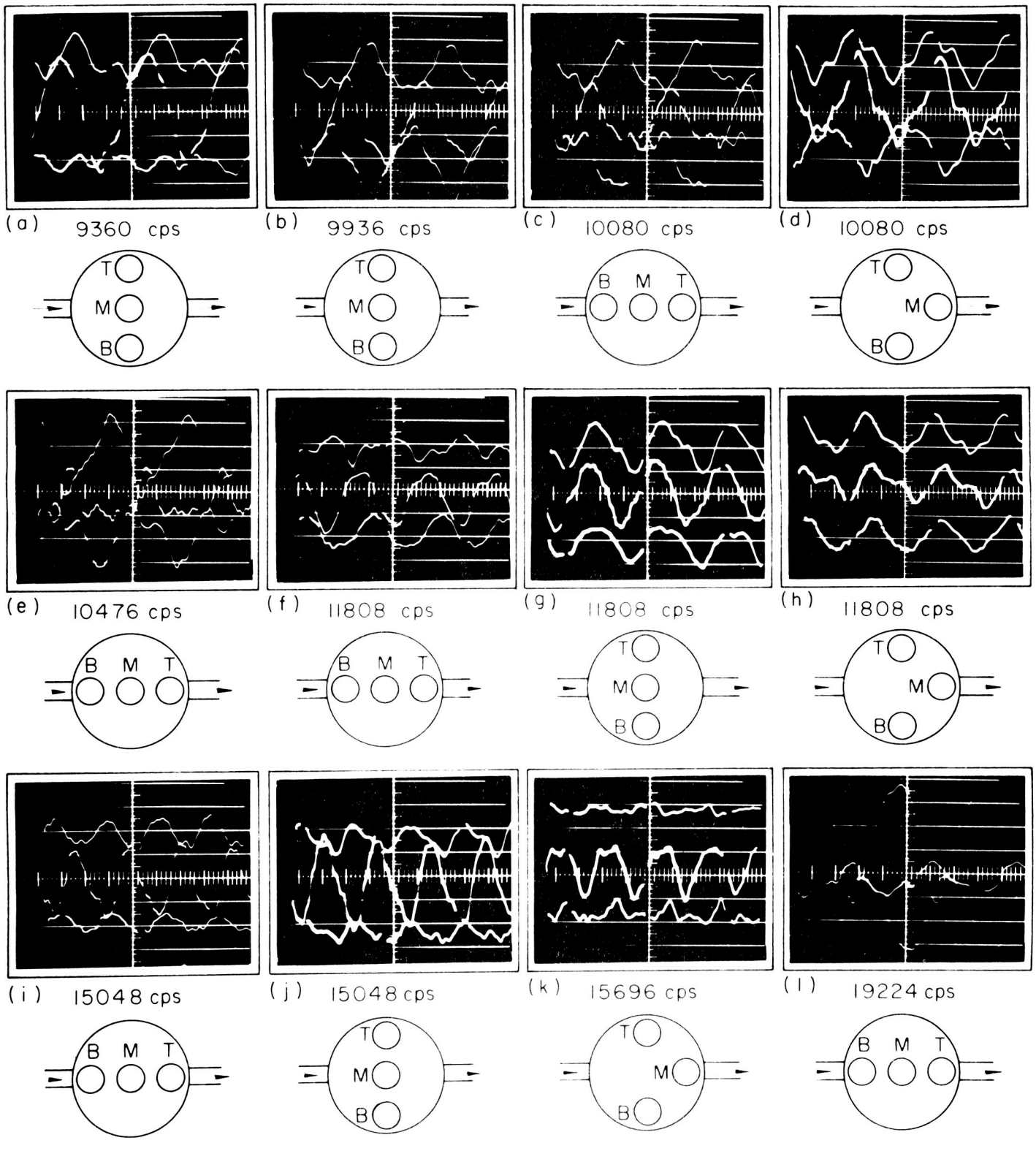

CHAMBER RESPONSE WITH FREON-12

FIGURE 18

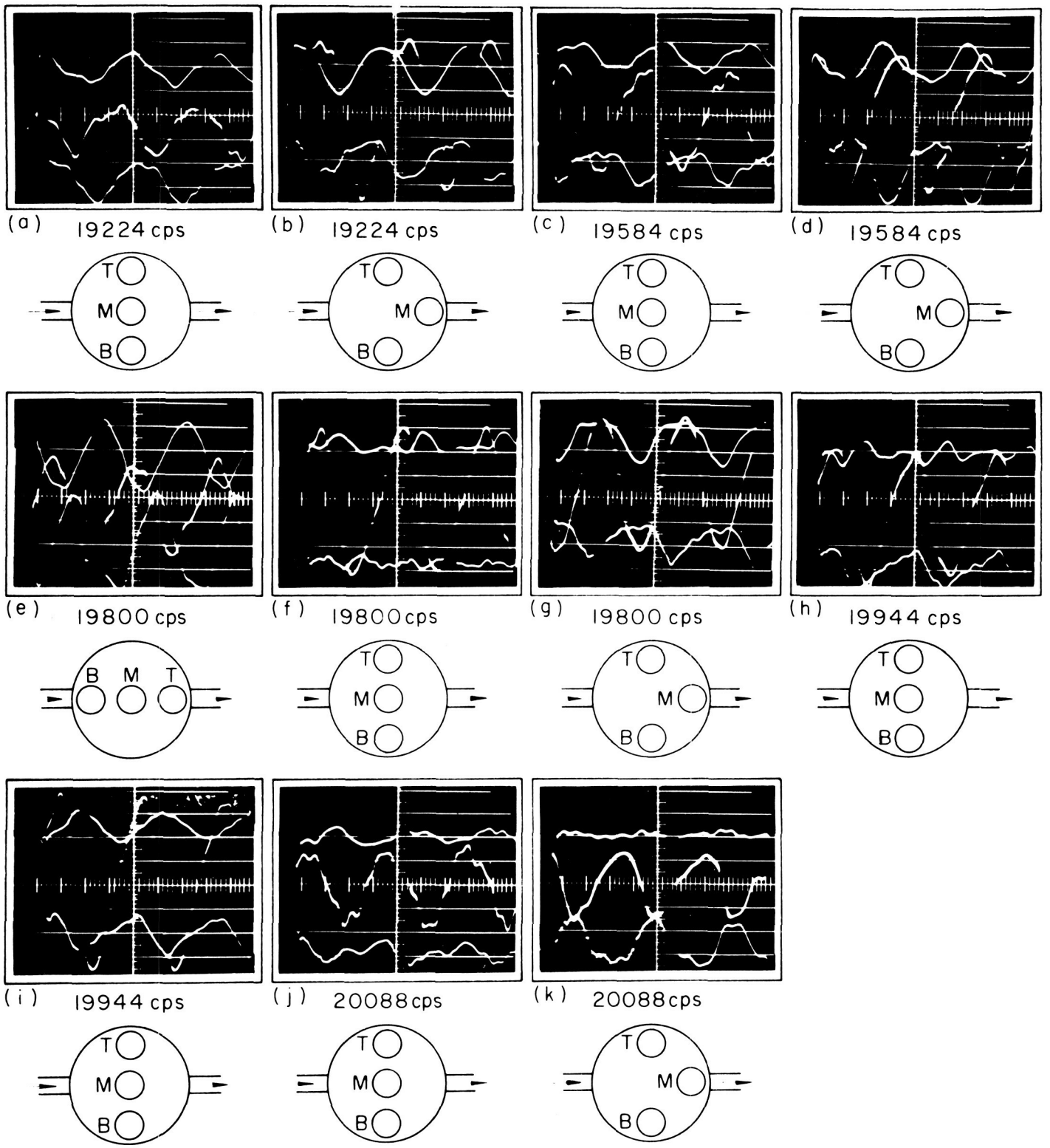

CHAMBER RESPONSE WITH FREON-12

FIGURE 19

gases. The resonant frequency is proportional to the velocity of propagation and thus to the square root of the temperature. To account for a ten percent frequency difference, however, the temperature would have to have been in error by approximately 100°R. This was very unlikely.

Another possibility was that the equation for the propagation of sound could not be used for the wave propagation velocity. The velocity of a finite pulse is always greater than the velocity of sound (infinitesimal pulse), but this would have made the calculated resonant frequencies even higher and thus in the wrong direction to account for the discrepancies.

An explanation for this discrepancy between the calculated acoustic resonant frequencies and the frequencies of finite amplitude resonances is given by Maslen and Moore (4), who show that a strong transverse wave has a lower frequency than the corresponding acoustic mode. The effect is, however, fairly small; e.g., if the maximum peak-to-peak pressure amplitude in the first (lowest frequency) transverse mode were one-third the chamber pressure, the frequency of the strong wave would be reduced from that of the associated sonic wave by less than two percent for γ = 1.4 (nitrogen). If the maximum peak-to-peak amplitude were one half the chamber pressure, then the pressure would be reduced less than three percent. Thus it is unlikely that this effect could have produced the observed discrepancy.

The first and second tangential modes were clearly dominant within their respective frequency ranges, but for the higher frequencies no pure mode was found to be dominant. The low "Q" (sharpness of resonance) of the chamber was demonstrated at the lower frequencies with both nitrogen and Freon-12. This permitted a pattern to exist over a wide frequency range, and therefore as the frequency increased, the "bunching" of resonant frequencies prevented the dominance of any one mode. This "bunching" of the

resonances at the higher frequencies can be illustrated by observing the Freon-12 resonances presented in the table on p. 37.

Although all of the combined modes are listed, the combined forms which include a longitudinal mode would appear on the end wall (in which the transducers were mounted) simply as the other component of the combined form. For example, a combined first tangential and first longitudinal would appear as a first tangential mode at $z = L$. The equation for the pressure at any particular location on the end wall can be obtained from

$$\varphi = (\cos\varphi)(\cos\pi)\, J_1\left(\frac{\pi\alpha_{10} r}{a}\right) e^{-\frac{\pi c \alpha_{10} i t}{a}} \qquad (30)$$

$$= -\cos\varphi\, J_1\left(\frac{\pi\alpha_{10} r}{a}\right) e^{-\frac{\pi c \alpha_{10} t}{a}}$$

Theoretically, then, the only combined form appearing as a combined form at the end wall would be a tangential-radial mode, and even this type of mode might be indistinguishable depending on the positioning of the transducers.

Some discussion of the more clearly defined pressure patterns at 9360 cps and above is of interest at this point.

At 9360 cps (18a) the pattern apparently indicated a radial mode. At 9936 cps (18b) and 10,080 cps (18c, d) elements of a first radial and a third tangential mode were present. The one photograph showing the response at 10,476 cps (18e) indicated that the response was primarily third tangential. The calculated resonant frequency for the third tangential mode was 11,380 cps. Note the progression in the waveform as the frequency was increased.

There are three photographs which present the response at 11,808 cps (18f, g, h). All the traces were in phase and equal in amplitude except for the photo showing the response of transducers

placed along a diameter in line with the inlet and discharge. The only applicable mode at this frequency was the first longitudinal, for which the calculated resonant frequency was 11,230 cps.

Between 11,808 and 15,048 cps the response was quite irregular, although of fairly large amplitude. At 15,048 cps (18i, j) both photographs clearly show that the predominant mode was radial. The response near the edge of the chamber was 180° out of phase with the center and of much lower amplitude. The calculated first-radial-mode resonant frequency was 18,950 cps, but the resonant frequency for a combined first radial and a first longitudinal was 15,320 cps.

Although the response from only one configuration of transducers was presented for 15,696 cps (18k) the pattern was a stabilized tangential mode, which could be identified from the location of the nodes as the fifth tangential mode. Its calculated resonant frequency was 17,380 cps.

At 19,224 cps (18ℓ, 19a, b), elements of various modes were present, an odd tangential and a longitudinal or a radial. The response at 19,584 cps (19c, d) was similar to that at 19,224 cps with the radial mode being more nearly dominant. This type of pattern persisted on up through 20,088 cps (19j, k).

The important conclusion to be derived from these data at the higher frequencies is that various modes can exist concurrently in the chamber, especially where the calculated resonances are close together.

C. Integrated Response of a Test Transducer

In Section III-B the response of a diaphragm transducer to known pressure patterns was discussed theoretically. Results of the attempted experiment verification are presented in this section.

The analysis predicted that a test transducer (e.g., one of the

Dynisco PT49 series) with a circular diaphragm should show no net response to tangential modes, but could show response to radial modes depending upon the effective area of the diaphragm as compared to the area of the chamber in which it was mounted.

The test transducer was mounted in the pressure generator, one quartz transducer was mounted in the opposite end wall and another in the curved side wall of the chamber.

The amplitudes of response of the transducers were adjusted so that all three traces on the oscilloscope had equal amplitudes when using helium at 4000 cps. All signals were fed through the three filters mentioned previously. The top trace on the photographs in Figure 20 is from the quartz reference transducer mounted in the center of the end wall, the middle trace is from the transducer mounted in the curved side wall, and the bottom trace is from the test transducer. All tests were conducted using Freon-12.

The test transducer showed low amplitude and distorted response at 4828 cps (20a). (The quartz transducer in the side wall verified the presence of the first tangential mode.) This compared well in both wave-shape and amplitude with the transducer in the opposite end wall, indicating the predicted response of the test transducer to a tangential pattern.

The behavior at 4828 cps was duplicated at 7128, 7200, and 7488 cps (20b, c, d), but was even more clear-cut, indicating that the response of the test transducer to the second tangential mode was very low.

It has therefore been shown both theoretically and experimentally that a test transducer of the flush diaphragm type is unaffected by tangential modes in the Sinusoidal Pressure Generator.

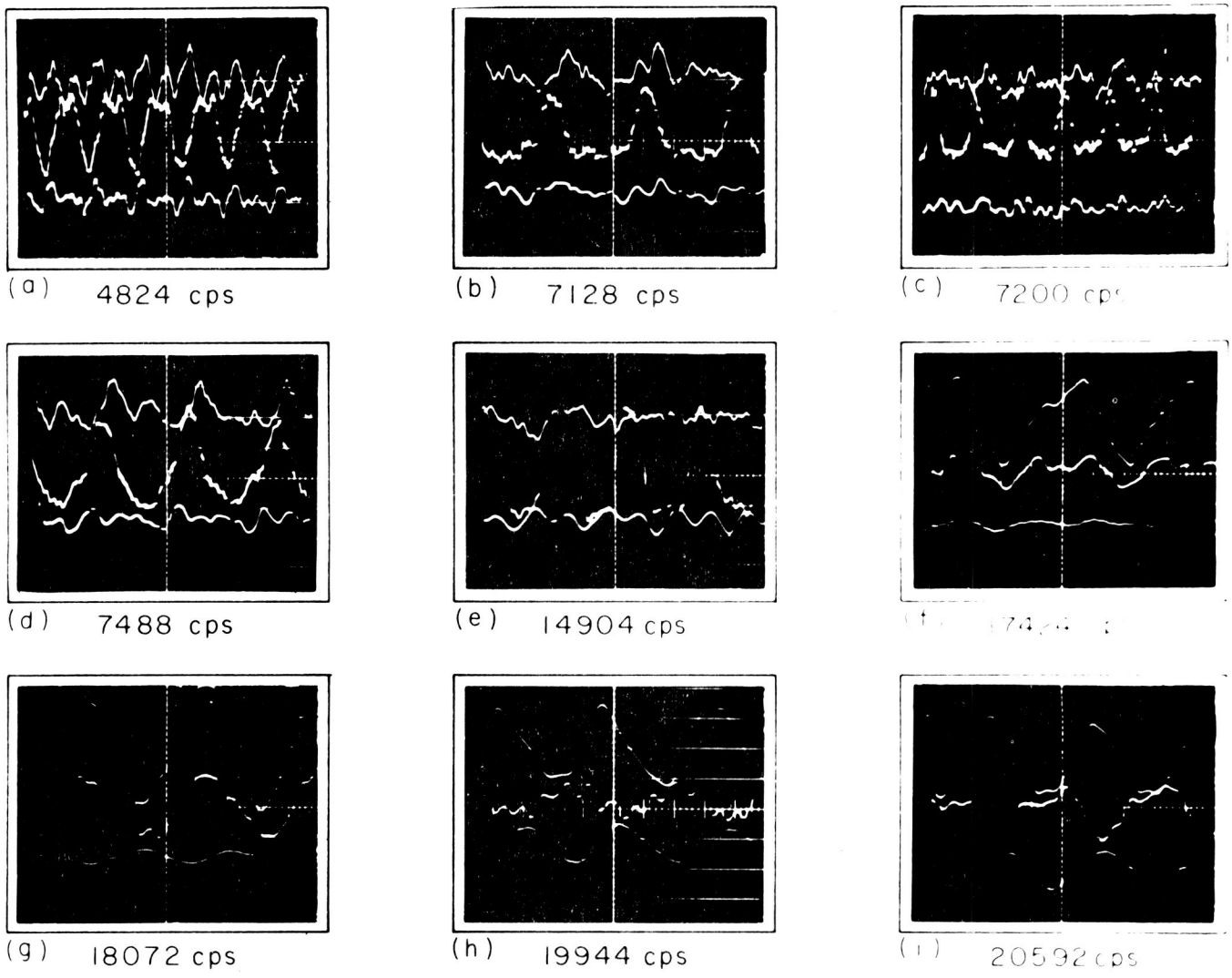

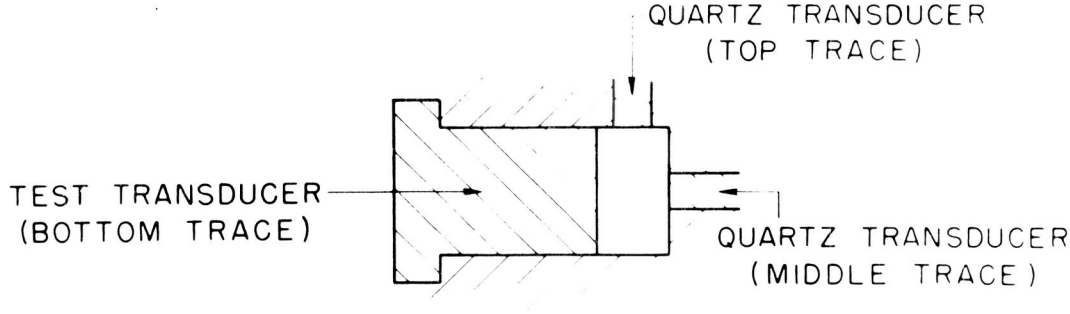

INTEGRATED TRANSDUCER RESPONSE WITH FREON-12

FIGURE 20

As the frequency was increased, an accurate classification of the patterns became more difficult especially with only two reference transducers as located in the chamber.

The pattern at 14,904 cps (20e) was clearly a tangential mode, since the center of the chamber exhibited low amplitude response while the transducer located in the side wall showed a high amplitude response. The low amplitude of the test transducer response further confirms the analytical predictions.

The pattern at 17,424 cps (20f) exhibited the characteristics of a radial mode, since the center and side wall transducers were in phase. This could not be true for a longitudinal mode. Although the test transducer response was quite low, it increased in direct proportion to the radial-mode amplitude at a higher frequency (18,072 cps - 20g). This supports the theoretical prediction of the response of a test transducer to a radial mode pattern.

VI. CONCLUSIONS

The sinusoidal pressure generator is useful as a transducer testing device up to about 10,000 cps in its present configuration using helium as the test gas (the use of hydrogen instead of helium would probably extend this range). The pressure amplitudes are adequate at all frequencies, but the response above 10,000 cps is increasingly non-uniform throughout the chamber.

The first and second tangential transverse modes were predictable by acoustic theory with the exception that the observed frequencies were somewhat lower than the calculated resonant frequencies. These results verify the theory of Maslen and Moore (4) that strong transverse waves can exist without shocks and that the frequencies for the strong waves tend to be lower than for the corresponding acoustic waves.

It was not possible to predict in advance the standing wave pattern at frequencies above the range of the second tangential mode. The ambiguity was caused by "bunching" of higher and combined modes due to the low "Q" (sharpness of resonance) of the cylindrical chamber.

Analytical predictions that test transducers having flat circular diaphragms exhibit little or no response to the tangential modes of chamber resonance were verified experimentally.

VII. RECOMMENDATIONS

It is recommended that further development of the Sinusoidal Pressure Generator and its operating technique be undertaken as follows:

A. Expand the operating frequency range -

   1. in the upper range from 10,000 to 15,000 cycles per second, and

   2. in the lower range down to 150 cycles per second.

B. Investigate the effect on performance of helium supply

   1. pressure and

   2. temperature.

C. Improve the design of the gas passages at the chamber

   1. inlet and

   2. discharge.

D. Evaluate the effect of changing the test gas from helium to

   1. hydrogen and

   2. other gases.

E. Investigate the difference between the theoretically and experimentally determined resonant frequencies of the chamber.

F. Measure in detail the effect of changes in chamber geometry.

G. Develop the transducer evaluation techniques associated with signal handling and display.

APPENDIX A: References

1. Jones, Howland B., Jr., "Transient Pressure Measuring Methods - Transient Pressure Transducer Design and Evaluation," Princeton University Aeronautical Engineering Report No. 595-b, February 1962.

2. Tallman, Charles R., "Transducer Frequency Response Evaluation for Rocket Instability Research,"

3. Morse, Philip M., "Vibration and Sound," McGraw-Hill Book Company, Inc., New York, 1948.

4. Maslen, Stephen H. and Moore, Franklin K., "On Strong Transverse Waves Without Shocks in a Circular Cylinder," Journal of the Aeronautical Sciences, vol. 23, no. 6, June 1956.

5. Reardon, Frederick H., "Combustion Instability in Liquid Rocket Motors - An Investigation of Transverse Mode Combustion Instability in Liquid Propellant Rocket Motors," Princeton University Aeronautical Engineering Report No. 550, June 1961.

APPENDIX B: Instrumentation Calibrations

Transducer Calibrations

All of the pressure transducers were calibrated statically using a dead weight calibration unit. The test transducer, a Dynisco PT49-IM series pressure transducer, was calibrated with its associated equipment, the D.C. amplifier and the regulated power supply. The response was linear even at the relatively low calibration pressures used. The results of this calibration are presented in Figure B-1.

The three quartz transducers and their amplifier-calibrators were also calibrated statically on the dead weight tester. The sensitivity of the system depended upon the length of the connecting cable from the transducer to the amplifier-calibrator. Two cable lengths were used. Results of the calibration are presented in Figure B-2.

Filter Characteristics

The circuit diagram of the three identical filters used is presented below.

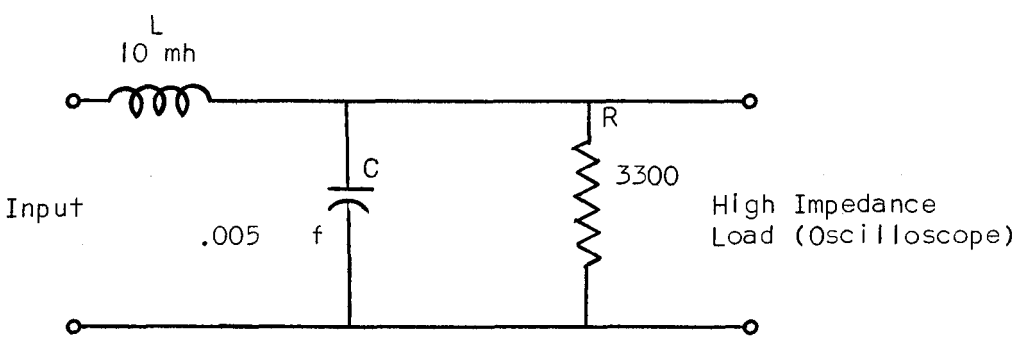

The phase shift and amplitude characteristics of these filters, presented in Figures B-3 and B-4, were determined in the following manner:

1. Amplitude - The amplitude of the sine wave output of a

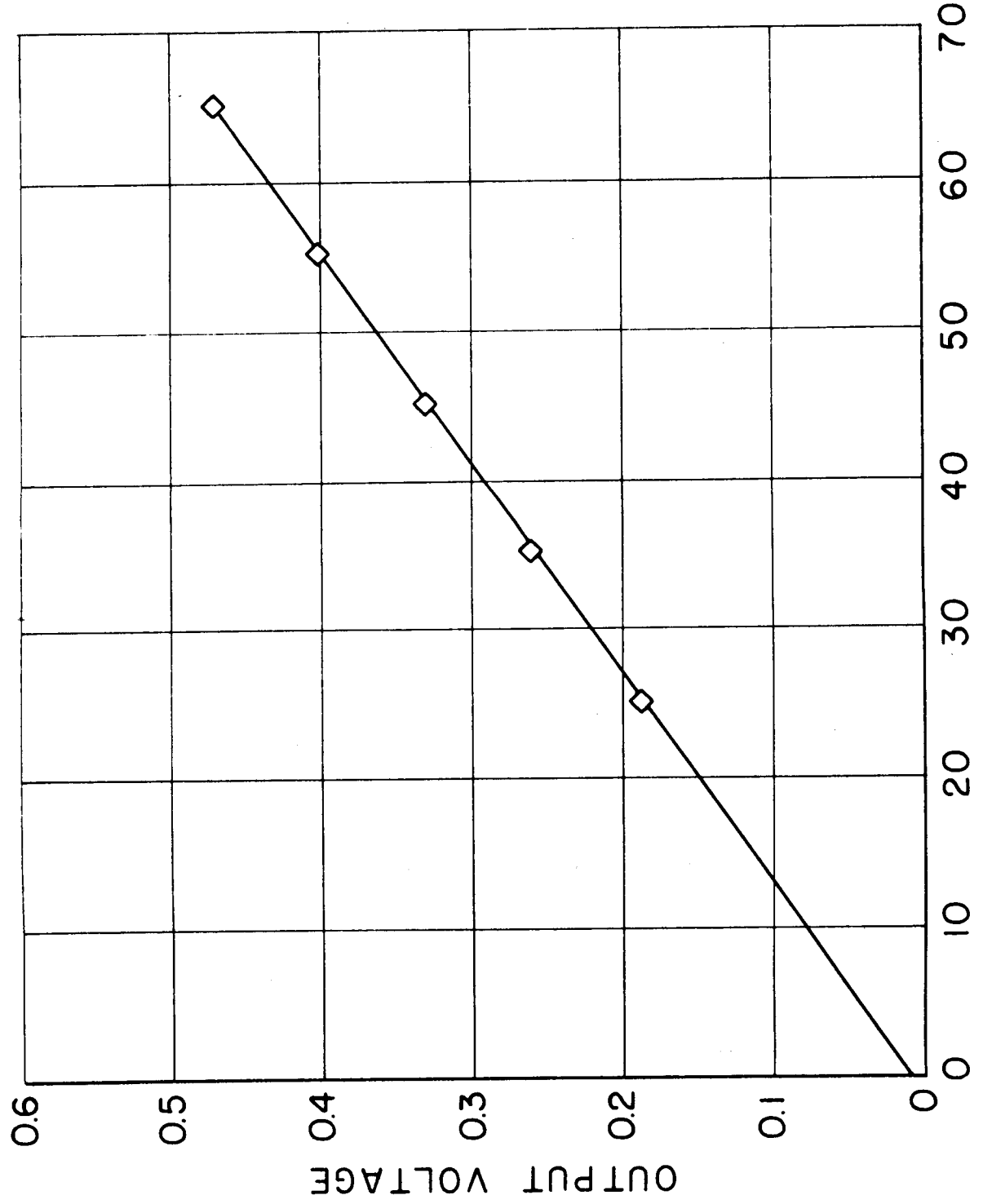
TEST TRANSDUCER CALIBRATION
APPLIED PRESSURE PSIG
OUTPUT VOLTAGE
0
10
20
30
40
50
60
70
0
0.1
0.2
0.3
0.4
0.5
0.6

FIGURE B-1

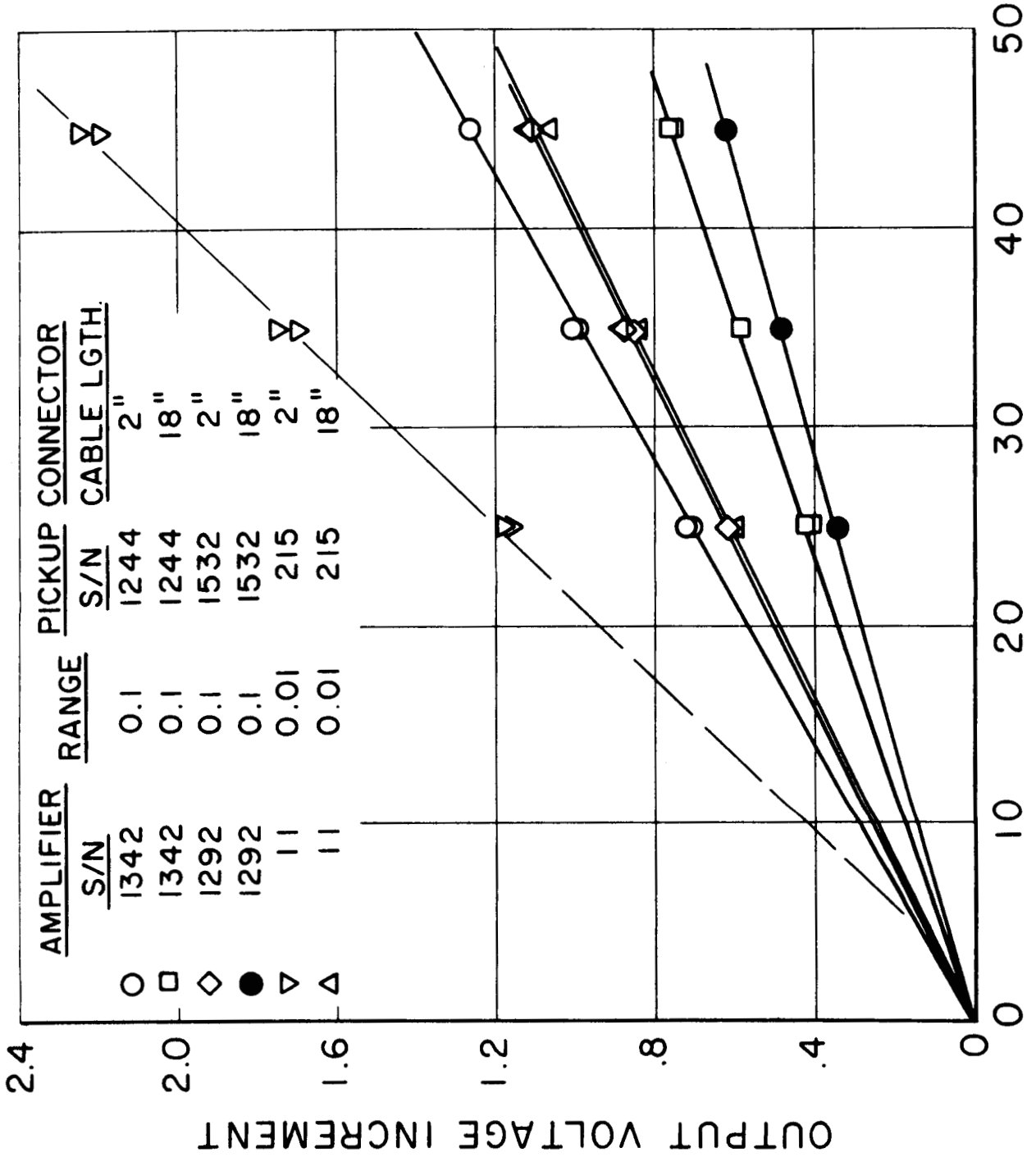

SENSITIVITY OF THE QUARTZ TRANSDUCER AMPLIFIER SYSTEMS

FIGURE B-2

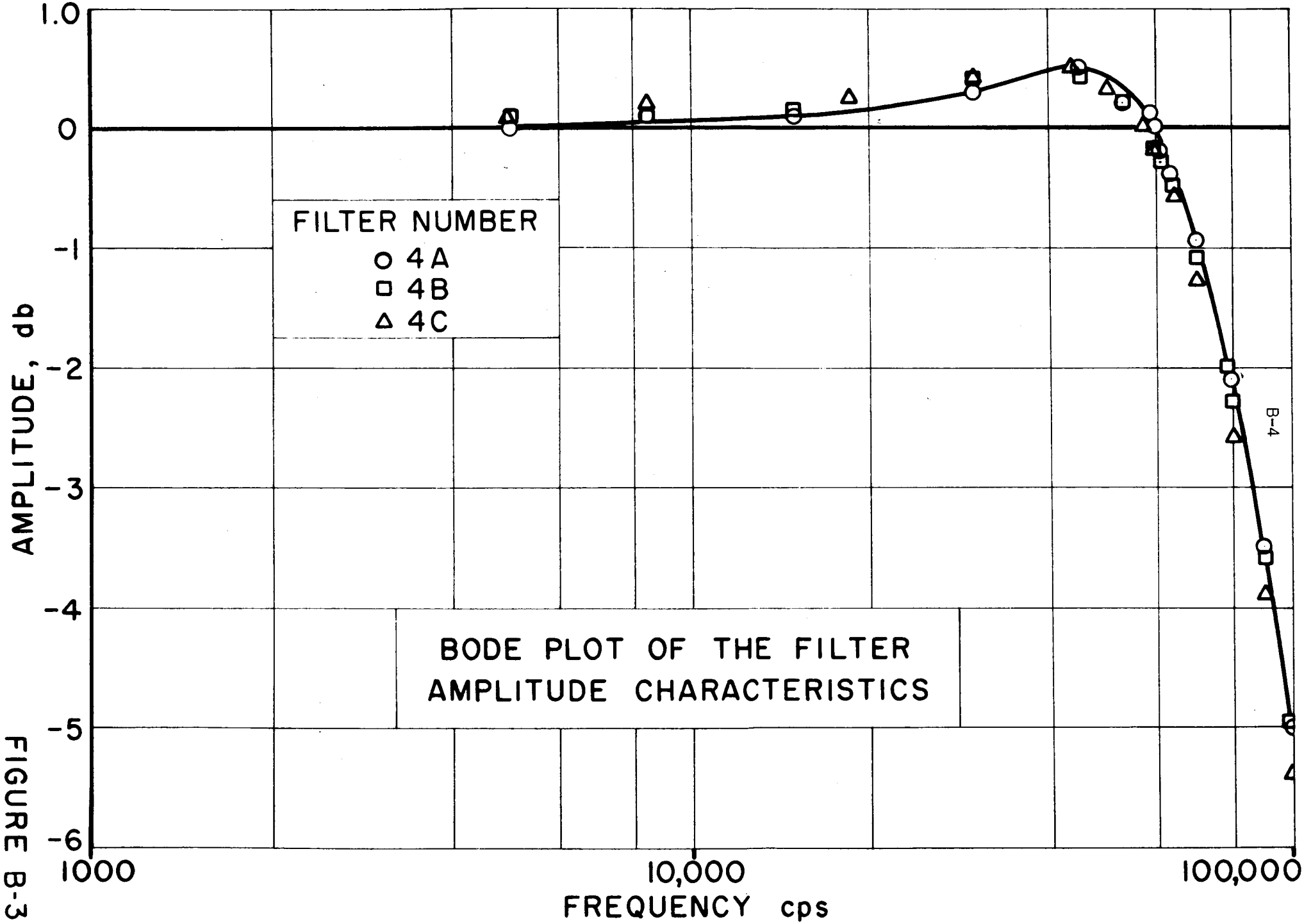
1.0
0
-1
-2
-3
-4
-5
-6
AMPLITUDE, db
FILTER NUMBER
4A
4B
4C
BODE PLOT OF THE FILTER
AMPLITUDE CHARACTERISTICS
B-4
1000
10,000
100,000
FREQUENCY cps

FIGURE B-3

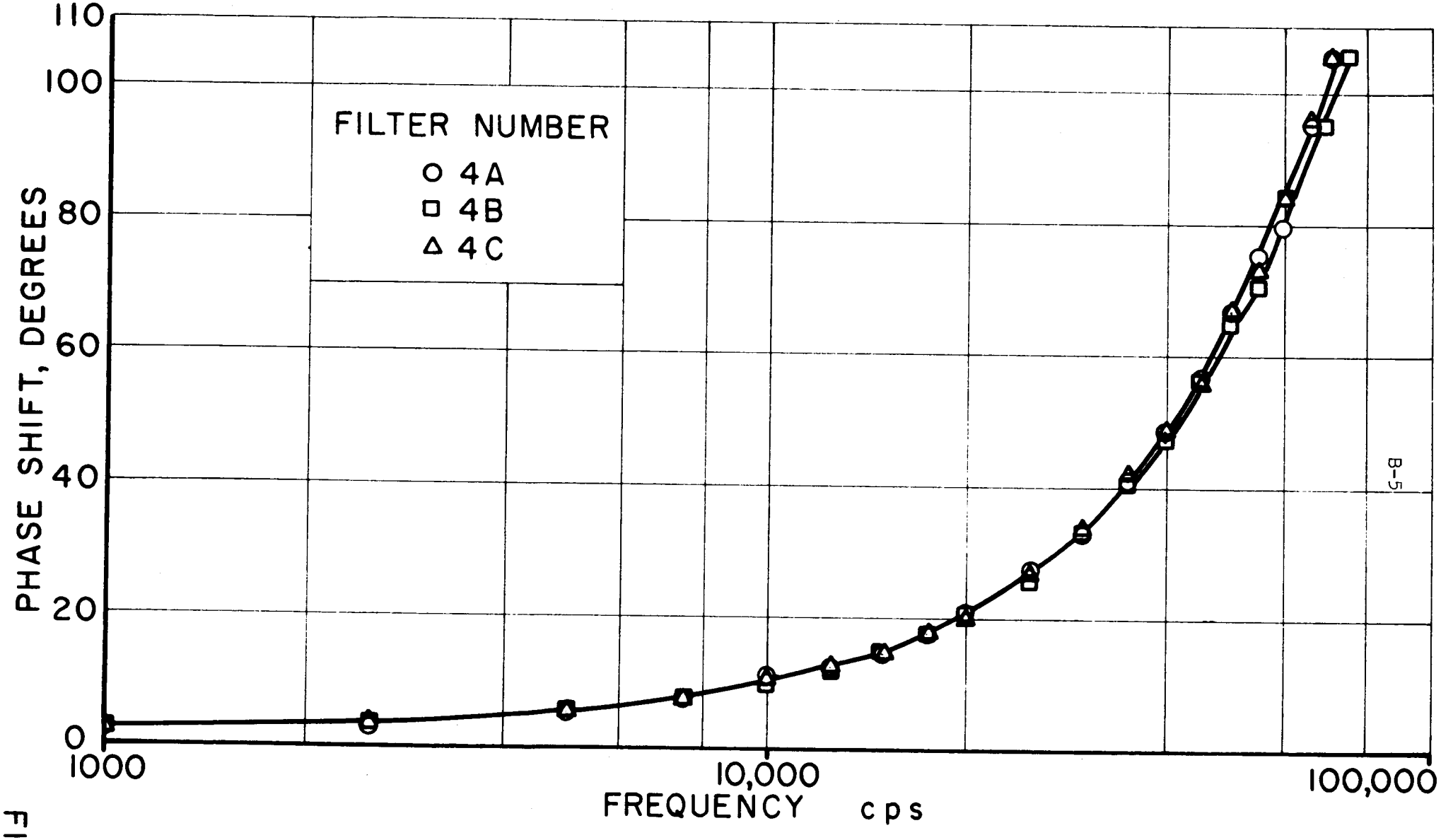

FIGURE B-4

BODE PLOT OF THE FILTER PHASE SHIFT CHARACTERISTICS

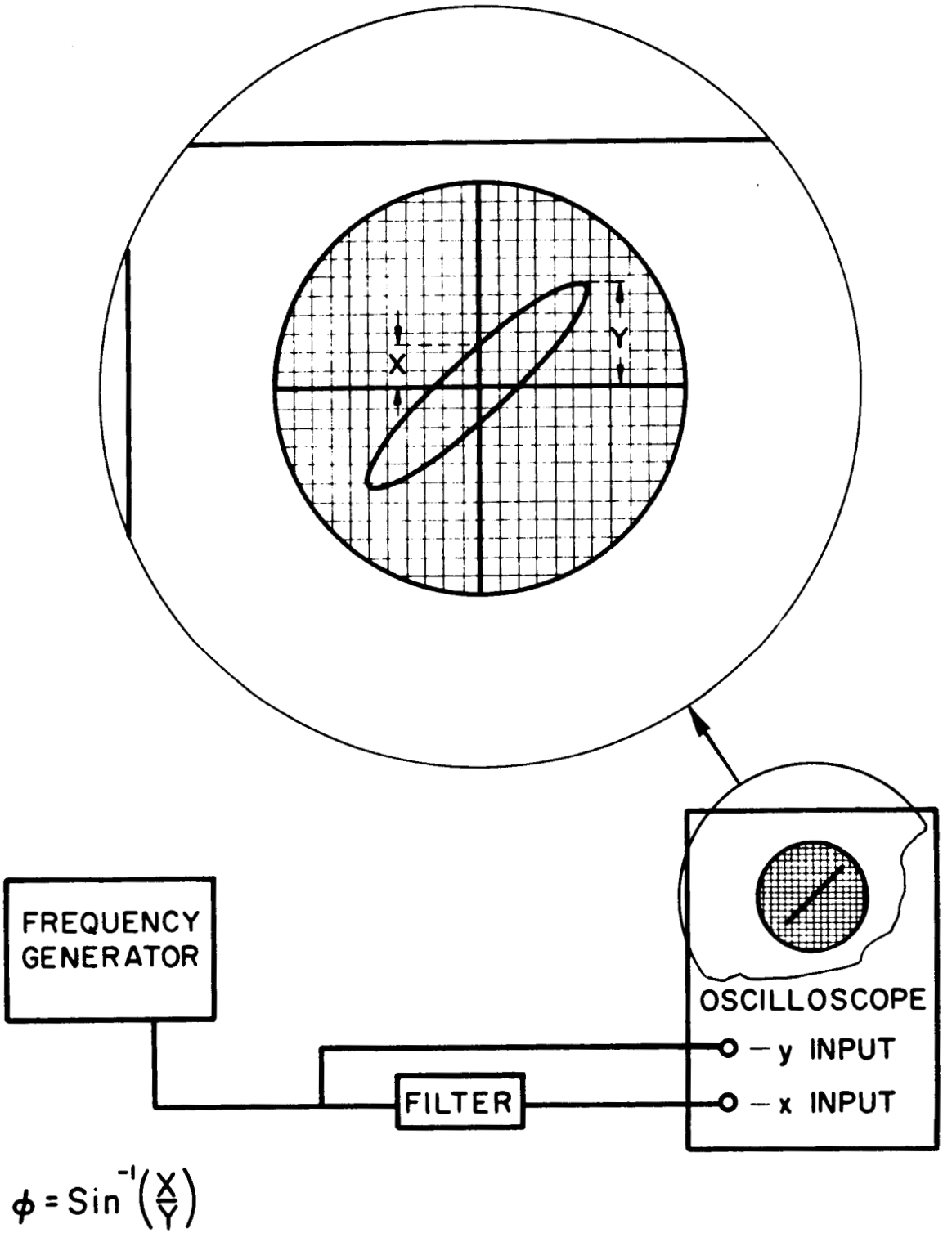

DETERMINATION OF FILTER PHASE SHIFT

FIGURE B-5

signal generator was set at 20 db. The filter was then inserted between the signal generator and the voltmeter. The db loss is plotted as a function of frequency in Figure B-3. The change in amplitude over the frequency range of interest (1800-21,600 cps) was small and no corrections were made to the data for the effect of filter insertion.

2. Phase Shift - Since three filters were used at all times, it is the phase shift between filters that is important. As can be seen from Figures B-4 this was fairly small. The phase shift was determined with the setup shown in Figure B-5 from which the phase shift can be calculated using the formula $\phi = \sin^{-1} X/Y$.

ITEM	MANUFACTURER	MANUFACTURER'S SPECIFICATION
1. Pressure Transducer Model 601 Minature Quartz Transducer	Kistler Instrument Company 15 Webster Street N. Tonawanda, New York	Pressure Range: 0-5000 psig Linearity: 1% of measured pressure Natural Frequency: 150,000 cps Rise Time: 3 μ sec.
2. Amplifier for 601 Transducer Model 655	Kistler Instrument Company	Input Signal (max): 1 volt Output Signal (max): 6 volts Gain (Adjustable): 3-6 Input Impedance: 10^{14} ohms Output Impedance: $<$ 100 ohms Linearity: 1% Response: 0-160,000 cps (3db point)
3. Pressure Transducer Dynisco PT 49F-1M S/N 9099	Dynisco Inc. 42 Carleton Street Cambridge 42, Mass.	Pressure Range: 0-1000 psig Natural Freq. (Nominal): 30,000 cps Max. Nonlinearity: 0.5% of full scale Max. Hysteresis: 0.5% full scale Repeatability: 0.1% of full scale
4. Strain Gage Power Supply Model SR-200-EHM	Video Instruments Inc. 3002 Pennsylvania Ave. Santa Monica, California	Regulation: 0.1%
5. D.C. Amplifier Model 71A	Video Instruments Inc.	Input-Differential or Single Ended Bandwidth: Within 1 db from D.C. to 20 kc D.C. Linearity: Better than $\pm$ 0.2% Gain Stability: 1% Zero Drift: less than 0.1% full scale output/hr. after warmup

ITEM	MANUFACTURER	MANUFACTURER'S SPECIFICATION
6. Oscilloscope and Amplifiers Model K-470	Electronic Tube Corp 1200 E. Mermaid Lane Philadelphia 18, Penna.	Model 470 Scope: 4 Gun cathode ray tube Vertical Amplifiers: Type 70A: Wideband high gain D.C. preamp Frequency Response - 10 cps to 5 mc at 50 mv/cm on A.C. coupling Type 70D: Similar to 70A but with greater sensitivity
7. Oscilloscope Camera Model 196A	Hewlett-Packard Palo Alto California	
8. Polaroid Land Film Type 47, 3000 Speed	Polaroid Corporation Cambridge 35, Mass.	
9. Electronic Voltmeter Model 310A	Ballantine Laboratories, Inc. Boonton, New Jersey	Accuracy: 3% from 10 cps to 1 mc Reads average voltage but scale calibrated to read rms voltage
10. D.C. Millivolt-meter Type MV-17B	Millivac Instruments Box 3027 New Haven, Connecticut	
11. Electronic Counter Eput Meter Model 7150	Berkeley Division Beckman Instruments, Inc. Richmond 4, California	Accurate to $\pm$ 1 count

ITEM	MANUFACTURER	MANUFACTURER'S SPECIFICATION
12. Varidrive	U.S. Electric Motors, Inc. Milford, Connecticut & Los Angeles, California	1.5 hp: 3 phase Type: VEUSESV-GH Minimum rpm: 1500 Maximum rpm: 6000 Motor rpm: 1800